NASA CR-72334
GEST-2101

TOPICAL REPORT

IRRADIATION OF HIGH PURITY ALUMINA

T. L. Gregory

prepared for

NATIONAL AERONAUTICS AND SPACE ADMINISTRATION

June, 1967

CONTRACT NAS 3-2544

Technical Management
NASA/Lewis Research Center
Cleveland, Ohio
Direct Energy Conversion Systems Branch
Jack F. Mondt

GENERAL ELECTRIC
PLEASANTON, CALIFORNIA

NASA CR-72334
GEST-2101

TOPICAL REPORT

IRRADIATION OF HIGH PURITY ALUMINA

by
T. L. Gregory

Prepared for
NATIONAL AERONAUTICS AND SPACE ADMINISTRATION

June 5, 1967

CONTRACT NAS 3-2544

Technical Management
NASA/Lewis Research Center
Cleveland, Ohio
Direct Energy Conversion Systems Branch
J. F. Mondt

GENERAL ELECTRIC COMPANY
Nuclear Thermionic Power Operation
Nuclear Technology Department
P.O. Box 846
Pleasanton, California

LEGAL NOTICE

TABLE OF CONTENTS

	Page
ABSTRACT	v
SUMMARY	1
INTRODUCTION	5
A. Electrical Insulator Requirements for Nuclear Thermionics	5
B. Technical Considerations - Literature Search	6
EXPERIMENTAL APPROACH	7
A. Irradiation Conditions	7
B. Material Characterization	7
1. Chemical Characterization	7
2. Metallographic Analyses	10
3. Electrical Properties	10
C. Capsule Design	10
D. Capsule Component Testing	13
1. Thermal Mock-Up of Capsule Sub-Assembly	17
2. Electrical Measurements of Lucalox	17
E. Capsule Instrumentation and Console	20
1. Instrumentation	20
2. Console	21
F. Capsule Fabrication and Check Out	21
1. Capsule Assembly	21
2. Capsule Test	24
G. Hazards Analysis	25
1. Hazards Considerations	25
2. Maximum Credible Accident	26
H. In-Pile Electrical Measurements	27

TABLE OF CONTENTS - (continued)

	Page
EXPERIMENTAL RESULTS AND DISCUSSION	30
A. In-Pile Electrical Measurements of Lucalox Alumina	30
B. Post-Irradiation Examination of Capsule	36
1. Internal Gas Pressure Measurement and Analysis	36
2. Visual Examination of Sample Assembly	37
3. Sample Disassembly and Visual Examination	38
4. Dimensional Measurements	43
5. Metallographic Examination	44
6. Flux Wire Scan and Analysis	46
APPENDIX A - OUT-OF-PILE TEST ON ALUMINA SPECIMENS	A-0
Thermal Mock-Up Test of Capsule Sub-Assembly	A-1
Out-of-Pile Electrical Resistivity Measurements of Lucalox	A-7
Four Probe Electrical Resistivity Measurements of Lucalox	A-8
Electrical Resistivity Measurements of Wesgo Alumina	A-10
APPENDIX B - DATA PLOTS OF IN-PILE MEASUREMENTS	B-0
REFERENCES	

LIST OF FIGURES

Figure No.	Title	Page
1	Lucalox Test Specimen	8
2	Cylindrical Section of the Specimen Showing Typical Porosity	11
3	Microstructure of the Cylindrical Section Showing Structure	11
4	High Purity Alumina Specific Resistance vs Temperature	12
5	Alumina Specimen and Holder Subassembly for Irradiation Experiment	14
6	Capsule Assembly for Lucalox Sample Irradiation	15
7	Gamma Heat vs Vertical Core Position and Location of Specimens	16
8	Parts of the Alumina Irradiation Capsule Showing the Eight Alumina Specimens, Electrodes, Vacuum Can and Seal Prior to Assembly	22
9	Alumina Specimens, Leads, and Vacuum Seal Prior to Installation in Vacuum Can	23
10	In-Pile Measurement Circuit Diagram	28
11	Resistivity vs Temperature for Various Exposures - Specimen No. 6	32
12	Resistivity vs Temperature for Various Exposures - Specimen No. 8	33
13	Alumina Irradiation Specimen Temperature Profiles During PBR Cycle No. 23	34
14	Neutron Exposure (nvt) >1 MeV vs Time in Reactor	35
15	Photographs of Specimens During Post-Irradiation Examination	39-40
16	Section of Typical Specimen Showing Porosity Unchanged Due to Irradiation	45
17	Photomicrograph of Lucalox-Kovar Interface Showing Reaction Zone - Typical of Specimens Stuck to Kovar Electrode	45
18	Gamma Activity Profile	47
A.1	Test Assembly	A-2

List of Figures - (Continued)

Figure No.	Title	Page
A.2	NASA Insulator Irradiation - Thermal Test Temperature Profile	A-5
A.3	Resistivity vs Temperature Measured During Thermal Test	A-6
A.4	Resistivity vs Temperature - NASA Insulator Assembly (isothermal test)	A-9
A.5	Electrical Resistivity of Wesgo 97.5	A-11
B.1	Resistivity vs Temperature for Various Exposures, Specimen No. 1	B-1
B.2	Resistivity vs Temperature for Various Exposures, Specimen No. 2	B-2
B.3	Resistivity vs Temperature for Various Exposures, Specimen No. 3	B-3
B.4	Resistivity vs Temperature for Various Exposures, Specimen No. 4	B-4
B.5	Resistivity vs Temperature for Various Exposures, Specimen No. 5	B-5
B.6	Resistivity vs Temperature for Various Exposures, Specimen No. 6	B-6
B.7	Resistivity vs Temperature for Various Exposures, Specimen No. 7	B-7
B.8	Resistivity vs Temperature for Various Exposures, Specimen No. 8	B-8

GEST-2101

IRRADIATION OF HIGH PURITY ALUMINA

ABSTRACT

In-situ measurements of electrical resistivity and voltage breakdown were performed on cylindrical specimens of high purity alumina. Eight specimens were irradiated in the NASA Plum Brook Reactor for 1290 hours at temperatures of 800 to 1000°C and received a fast neutron (> 1 MeV) dose of 1.4 to 1.6 x 10^{20} nvt. Data of the pre-irradiation and in-situ electrical measurements are reported and analyzed; the results of the post-irradiation examination of the specimens are presented.

IRRADIATION OF HIGH PURITY ALUMINA

SUMMARY

Insulator materials for nuclear thermionic applications must have properties to satisfy such characteristics as: chemical compatibility with cesium vapor and refractory metals; coefficient of thermal expansion similar to that of certain refractory metals; high electrical resistivity and voltage breakdown; resistance to radiation damage; and good fabricability. A candidate material for this application is high purity alumina (Al_2O_3). The effects of the nuclear environment on the electrical characteristics, dimensional stability and thermal-mechanical integrity must be known and an irradiation program was performed accordingly.

The objective of this program was to obtain engineering data on high purity alumina properties as a function of exposure in a nuclear environment with the test conditions being consistent with those required in thermionic applications.

High purity (99.5%) alumina specimens, nontranslucent high-strength-grade Lucalox was used in the experiment. Chemical and metallographic analysis was performed prior to irradiation. The only significant impurity detected was 5000 ppm of magnesium (used as a densification additive). The material was single phase alpha with a small amount of isolated porosity and a uniform grain size with an average grain diameter of approximately 0.0005 inch. The specimen dimensions were 0.750 inch in length, 0.625 inch outside diameter and a wall thickness of 0.030 inch. A lip of approximately 1/16 inch was incorporated in the design of the specimen to facilitate mechanical assembly.

The irradiation capsule was designed to accommodate eight alumina specimens. The capsule assembly consisted of an inner electrode of Kovar,

the Lucalox specimen, and an outer molybdenum electrode. Located immediately outside the molybdenum electrode were four segments of high purity alumina serving as isolation insulators, which were supported by fluted stainless steel retainers which also served as controlled heat conduction paths. The capsule instrumentation consisted of the continuous common Kovar electrode, a nickel electrode measurement wire that was welded to each of the molybdenum electrodes and the common center electrode. A nickel flux wire was inserted down the center hole of the Kovar inner electrodes. Four Inconel sheathed Pt. vs Pt-13% Rh thermocouples were used to measure four of the inner electrode temperatures during operation. The entire assembly was contained in a stainless steel tube $\sim$ 40 inches long in order that the vacuum-tight electrical feed-through consisting of 15 individual ceramic-to-metal seals be positioned in a low temperature, low neutron flux region. A dummy electrical lead was installed in the ceramic-to-metal seal along with a thermocouple to measure the lead and seal leakage so this could be subtracted from the measurements made on the specimen. The main source of heat was provided by the gamma heat of the reactor. An electrical heater was located on the outside of the stainless steel vacuum container to provide a fine temperature control. A stainless steel containment provided the barrier between the vacuum container and the reactor coolant. Helium gas at about 175 psi provided the heat transfer medium from the vacuum container to the reactor coolant.

All temperatures were recorded on a multi-point recorder. Leakage current through the alumina specimens were measured by an electrometer. Direct current voltage was applied by a regulated power supply. The trim heaters in the capsule were powered by a variable transformer. The voltage from the common center electrode to each individual outer electrode was supplied by the power supply through a selector switch to select the electrode for individual measurements. The currents from the instrumentation leads were measured with an electrometer circuit. The lead resistances were on the order of 10^6 ohms, while the resistance of the ceramic-to-metal

feed-through was on the order of 10^5 ohms higher than the specimen resistance at temperature.

An instrumented mock-up of a single specimen assembly was fabricated and tested out-of-pile in a vacuum bell jar. The purpose of this test was to determine the heat transfer characteristics and the adequacy of the capsule design. The test results indicated that the heat transfer and capsule design were satisfactory. During this test, electrical resistivity measurements were performed on the alumina specimen. There was scatter in the data points; however, the results compare favorably with published data. Typical values are presented in Table I below.

TABLE I

Electrical Resistivity Values* of Alumina (ohm-cm)

	Temperature, °C		
	600	800	1000
Lucalox Test (out-of-pile)	3×10^9	1×10^8	1×10^7
Published Data	2×10^9	3×10^7	2×10^6

(*Average values in the scatter band of data)

During the irradiation, measurements were made of electrical resistivity and breakdown voltage characteristics. The irradiation facility provided a fast flux of approximately 4×10^{13} nv with neutron energies greater than 1 MeV, and a thermal flux of 2×10^{14} nv. The gamma heating was in the range of 4 to 6 watts per gram. Specimen test temperatures ranged from 800 to 1000°C during the course of the irradiation. The in-pile electrical resistivity was approximately a factor of five (5) higher than the out-of-pile data. However, the slope of the electrical resistivity plotted as a log function of temperature is the same for in-pile and out-of-pile data. The test data also indicate that for the total exposure of 1290 hours, the total integrated neutron dose did not appear to change the resistivity of the specimens. The total fast integrated

neutron flux was approximately 1.6×10^{20} nvt for the highest exposure to about 1.4×10^{20} nvt for the lowest exposure. With the exception of one specimen, there was no evidence of voltage breakdown when 300 V d.c. was applied to each specimen. In one specimen at an exposure of 1×10^{20} nvt, a 1/8 ampere fuse in series with the electrode measurement line failed at 270 volts indicating an electrical breakdown. After the fuse was replaced, the same events occurred. However, electrical resistivity measurements performed on the specimen resulted in values identical to those obtained prior to the failure of the fuse. Post-irradiation examination failed to yield any evidence of an electrical breakdown of the alumina.

Post-irradiation examination was performed on the capsule. Visual observations and examination of the capsule exterior revealed that the heater, instrumentation and lead vacuum seal were not damaged. The capsule was disassembled and internal capsule surface and components were clean. All of the alumina, Lucalox specimens had turned from the characteristic milky white appearance to a dark gray color. The alumina isolation insulator also experienced a darkening but not to the same dgree as the Lucalox. The change in color of the alumina material is believed to be associated with the production of F or V color center irradiation defects. With the exception of one sample in which some breakage of the alumina was observed as a result of slight misalignment, all the alumina appeared to be crack free while in the electrode assemblies. Upon removal of the Lucalox specimens from the electrode assemblies, three of the specimens were bonded to the Kovar electrodes and of these three, two specimens had evidence of cracking. Of the five specimens that were freely removed from the electrode assemblies, four of them were crack-free while the remaining specimen had a circumferential fracture at the internal flange. A comparison of the pre- and post-dimensional measurements revealed no change. Metallographic observations of the alumina did not reveal any irradiation changes in the microstructure.

INTRODUCTION

A. Electrical Insulator Requirements for Nuclear Thermionics

The nuclear thermionic space power systems require electrical insulator materials which must meet a unique set of requirements of physical properties. Examination of available data[12, 6, 15, 20] for ceramic electrical insulators for use in thermionic and nuclear environments has shown that alumina is a natural choice for a number of reasons. Alumina has good compatibility characteristics with refractory metals[16, 4, 13, 31] such as tungsten and molybdenum; it has a good match of thermal expansion with niobium [6, 20]; it has high electrical resistivity, and thermal conductivity, and it has no phase changes at the required operating temperatures[31]. Much industrial experience has been gained from the wide use of this material in ceramic-to-metal seals and in cesium vapor environments[31]. Data were not available on the electrical resistivity and breakdown voltage while operating a high neutron flux at temperatures from 800 to 1000°C.

A program was therefore initiated to irradiate high purity alumina in the temperature range of 800 to 1000°C in order to obtain engineering design data[51, 52]. The program objectives were as follows:

1. To design and fabricate a capsule for the irradiation of eight high purity alumina specimens in the Plum Brook Reactor.

2. To determine the effects of irradiation on the electrical characteristics of the alumina. To perform in-situ measurements of electrical resistivity and voltage breakdown characteristics at elevated temperature.

3. To perform post-irradiation examination of the alumina and to determine the effects of radiation on the dimensional stability.

B. Technical Considerations - Literature Search

In nuclear thermionics, an electrical insulator material is needed between the collector and outer metallic sheath which is exposed to the reactor coolant. In addition, there are other requirements for the insulator material such as radial and axial spacers and intercell shields. To build up the voltage of the reactor systems, the thermionic cells must be connected in electrical series. This places an important set of requirements on the electrical sheath insulator material; high electrical resistivity at operating temperatures in the presence of a nuclear environment, adequate dielectric strength, compatibility with refractory metal components, thermal expansion match with the metallic sheath member, and ease of fabrication. With these demanding requirements, the selection of suitable insulator materials becomes limited. One insulator material that appears to best satisfy these requirements and which has been widely used in thermionics is high purity alumina.

While out-of-pile data on the electrical resistivity and voltage breakdown characteristics were available, a search of the literature yielded no information on these properties with both high temperature and neutron flux exposure.

EXPERIMENTAL APPROACH

A. Irradiation Conditions

The alumina insulator test conditions, configuration, temperature, and electrical voltage gradients selected were representative of design conditions anticipated for nuclear thermionic applications. A capsule containing eight specimens of high purity alumina (Lucalox) was designed to be tested in the Plum Brook Reactor under the following conditions:

1.	Temperature	800 - 1000°C
2.	Environment	vacuum 10^{-5} - 10^{-6} mm Hg
3.	Flux	$> 10^{14}$ nv thermal
		$> 10^{13}$ nv fast > 1 MeV
4.	Exposure Rate	$> 10^{19}$ nvt/day thermal
5.	Total Exposure	$> 10^{20}$ nvt fast > 1 MeV
6.	Gamma Heat	4 to 6 W/g
7.	Voltage Gradient	2 to 5 V/mil
8.	Test Position	LD-11 and LA-11

B. Material Characterization

The high purity alumina selected for this irradiation experiment was a nontranslucent high strength grade of GE "Lucalox". A typical Lucalox specimen is shown in Figure 1. Prior to irradiation, one Lucalox specimen was analyzed by spectrographic and metallographic technique.

1. Chemical Characterization

The chemical composition is presented in Table I. The spectrographic analysis was performed on two different areas of one specimen and was characteristic of Lucalox alumina. The only significant impurity observed was Mg (in solution in the Al_2O_3) which was present at 5000 ppm.

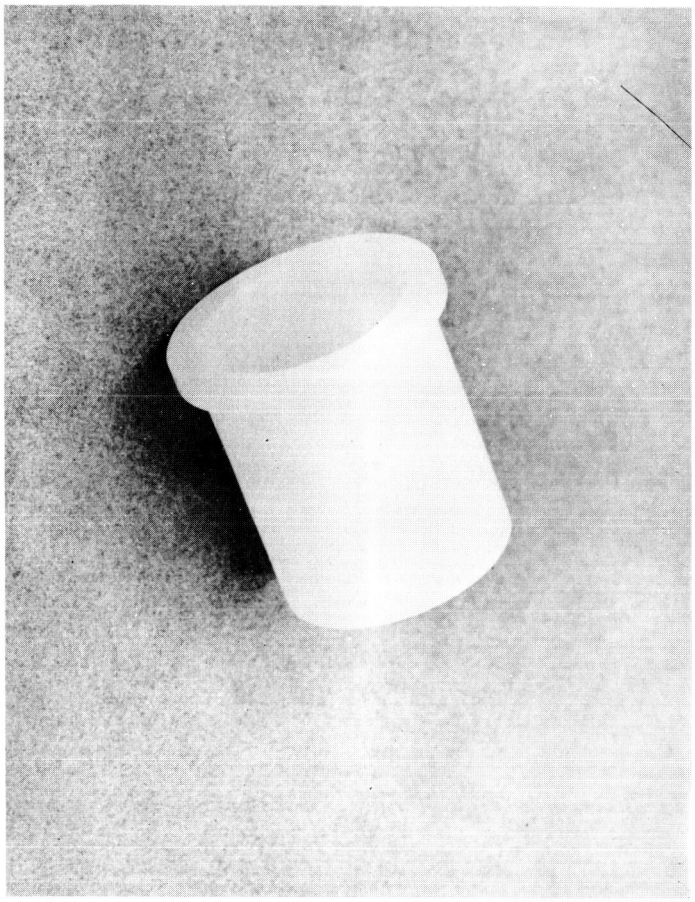

Figure 1. LUCALOX TEST SPECIMEN

TABLE I

Chemical Composition of Lucalox

	Area 1	Area 2
Ca	< 1 ppm	< 1 ppm
Co	< 10	< 10
B	< 10	< 10
Mg	5,000	5,000
Mn	< 10	< 10
Pb	< 10	< 10
Si	100	100
Fe	< 10	< 10
Cr	< 10	< 10
Ni	< 10	< 10
Bi	< 50	< 50
Al	Major	Major
Mo	< 10	< 10
Sn	< 50	< 50
V	< 10	< 10
Cu	< 1	< 1
Cd	<100	<100
Ag	< 1	< 1
Zn	< 50	< 50
Na	< 50	< 50
Sb	< 10	< 10
Ba	< 10	< 10
Ti	< 10	< 10
Cb	<100	<100
Sc	< 10	< 10
Y	< 10	< 10
K	< 10	< 10

2. Metallographic Analyses

Only alpha phase alumina was observed metallographically. The specimen was slightly more porous than transluscent Lucalox. The porosity in the cylindrical part of the specimen is illustrated in the ceramograph of Figure 2. The pores in the lip were somewhat larger in size; however, this porosity was not expected to significantly affect the electrical conductivity of the body when compared to 100% dense Lucalox.

The Lucalox specimen was etched to reveal the grain boundaries and a typical microstructure is illustrated in Figure 3. The grains were relatively small and typical of the "high-strength" grade of Lucalox. The grain size is uniform throughout the entire body; the average grain diameter is about 0.0005 inch.

3. Electrical Properties

Data on the specific resistance as a function of temperature for Lucalox were obtained from the vendor;[25] the data are plotted in Figure 4, along with data on high purity alumina obtained from other references.[6, 4, 20] As seen from this figure, the Lucalox data falls in a band which is typical for published data on electrical properties of alumina. Resistivity measurements were performed on the Lucalox specimens used in this experiment and the results are presented in the following section.

C. Capsule Design

In order to obtain a symmetrical heat distribution for the gamma heated alumina specimens and to achieve a good electrical and thermal contact with the specimen at the operating temperatures of the experiment, a cylindrical specimen geometry was selected for the capsule design. This design approach is also consistent with the requirement of testing representative nuclear thermionic components.

Figure 2. CYLINDRICAL SECTION OF THE SPECIMEN SHOWING TYPICAL POROSITY. AS-POLISHED, 100X

Figure 3. MICROSTRUCTURE OF THE CYLINDRICAL SECTION SHOWING GRAIN STRUCTURE. ETCHED, 150X

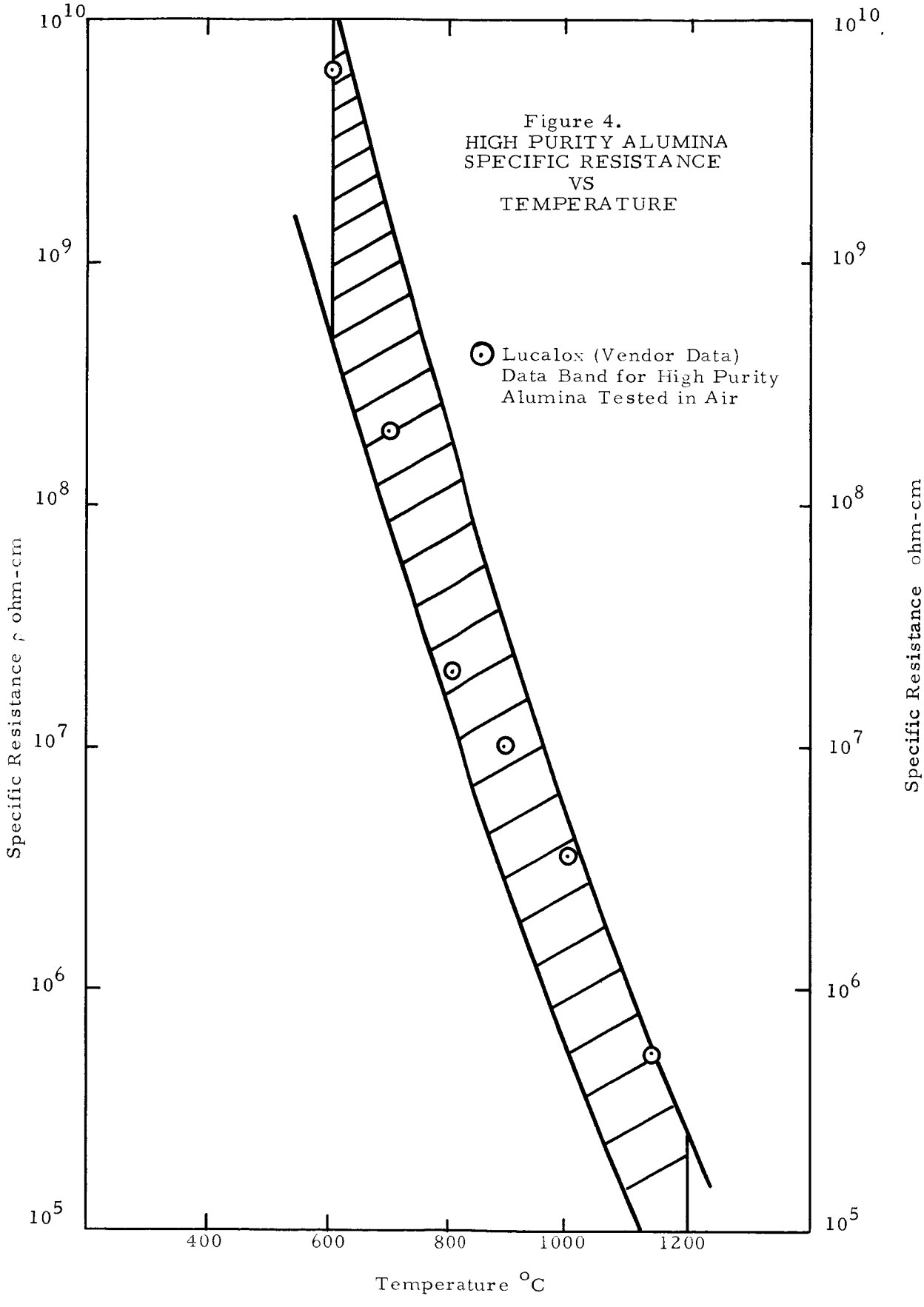
Figure 4.
HIGH PURITY ALUMINA
SPECIFIC RESISTANCE
VS
TEMPERATURE
Lucalox (Vendor Data)
Data Band for High Purity
Alumina Tested in Air
Specific Resistance ρ ohm-cm
Specific Resistance ohm-cm
10^{10}
10^{9}
10^{8}
10^{7}
10^{6}
10^{5}
400
600
800
1000
1200
Temperature °C

The capsule design analysis included heat transfer, mechanical and thermal stress, gamma heat distribution the core, electrical circuitry and proper selection of electrode materials. The capsule subassembly configuration that evolved from this analysis is shown in Figure 5. The specimen assembly consisted of an inner Kovar electrode selected to match the thermal expansion of alumina, the alumina specimen with an end lip designed to assist in mechanical assembly of the capsule and to minimize electrical leakage across the ends of the specimens, a molybdenum outer electrode, four segments of an electrical isolation insulator, a finned-stainless steel thermal conduction member, a stainless steel container and a stainless steel capsule container. The selection of electrode materials was based on chemical compatibility with alumina, and a thermal expansion match with alumina such as to provide sufficient contact to minimize thermal and electrical contact resistance.

The irradiation capsule consisted of eight Lucalox specimens and the sub-assembly specimen holders. A drawing of the longitudinal section of the capsule is shown in Figure 6. Irradiation of the capsule was scheduled for position LA-11, the corner of the active region of the core in the Plum Brook Reactor Facility (PBRF). Data on the gamma heat generated in this position as a function of critical core position were provided by the PBRF Project Engineer and are shown in Figure 7. These data provided the basis for the heat transfer analysis in the capsule design.

D. Capsule Component Testing

Several capsule component tests were performed to verify the capsule design analysis. These tests included a thermal mock-up of the specimen electrode sub-assembly, electrical resistivity of alumina and an evaluation of electrical contact resistance. The tests and the results are summarized herein. A more detailed description of the experiments and discussions are included in the appendix.

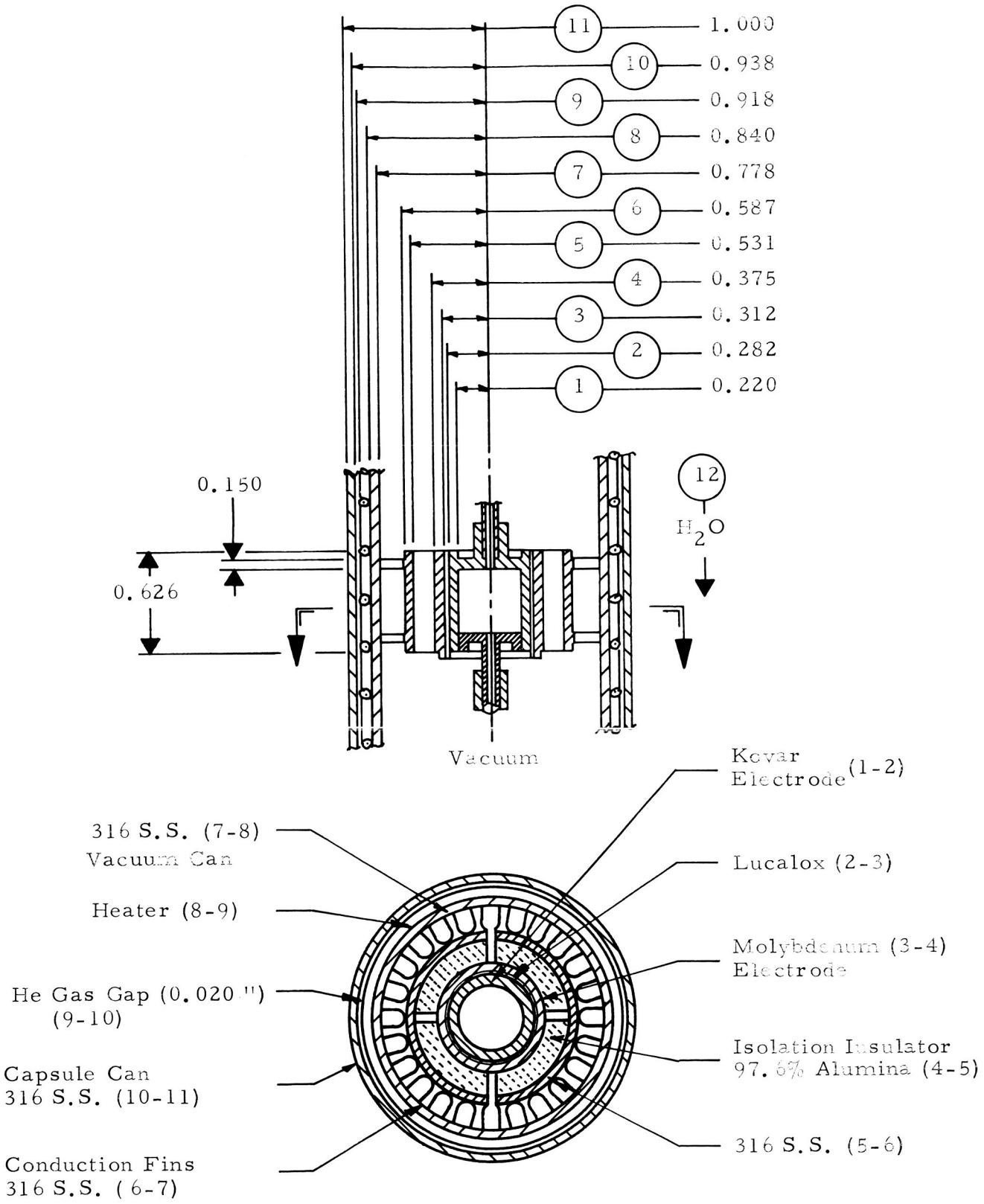

Figure 5. ALUMINA SPECIMEN AND HOLDER SUBASSEMBLY FOR IRRADIATION EXPERIMENT

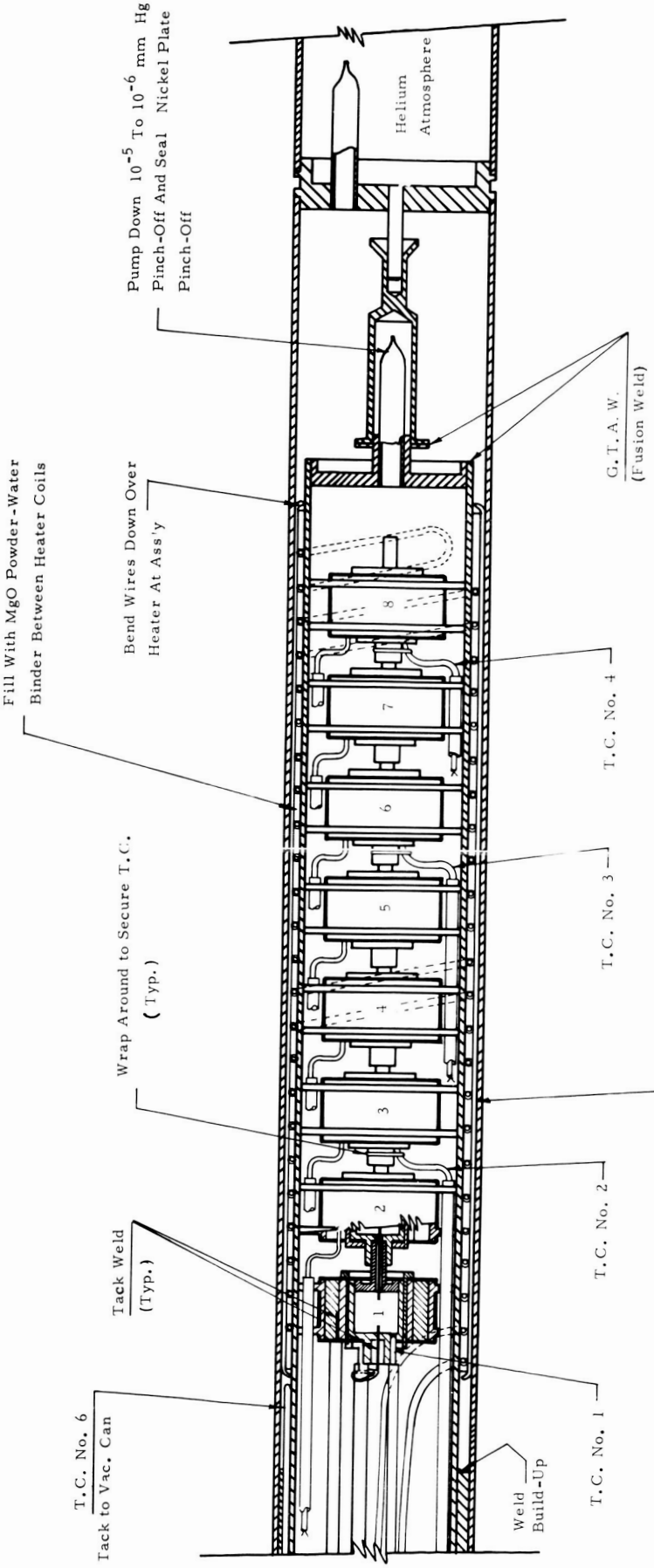

FIGURE 6 CAPSULE ASSEMBLY FOR LUCALOX SAMPLE IRRADIATION

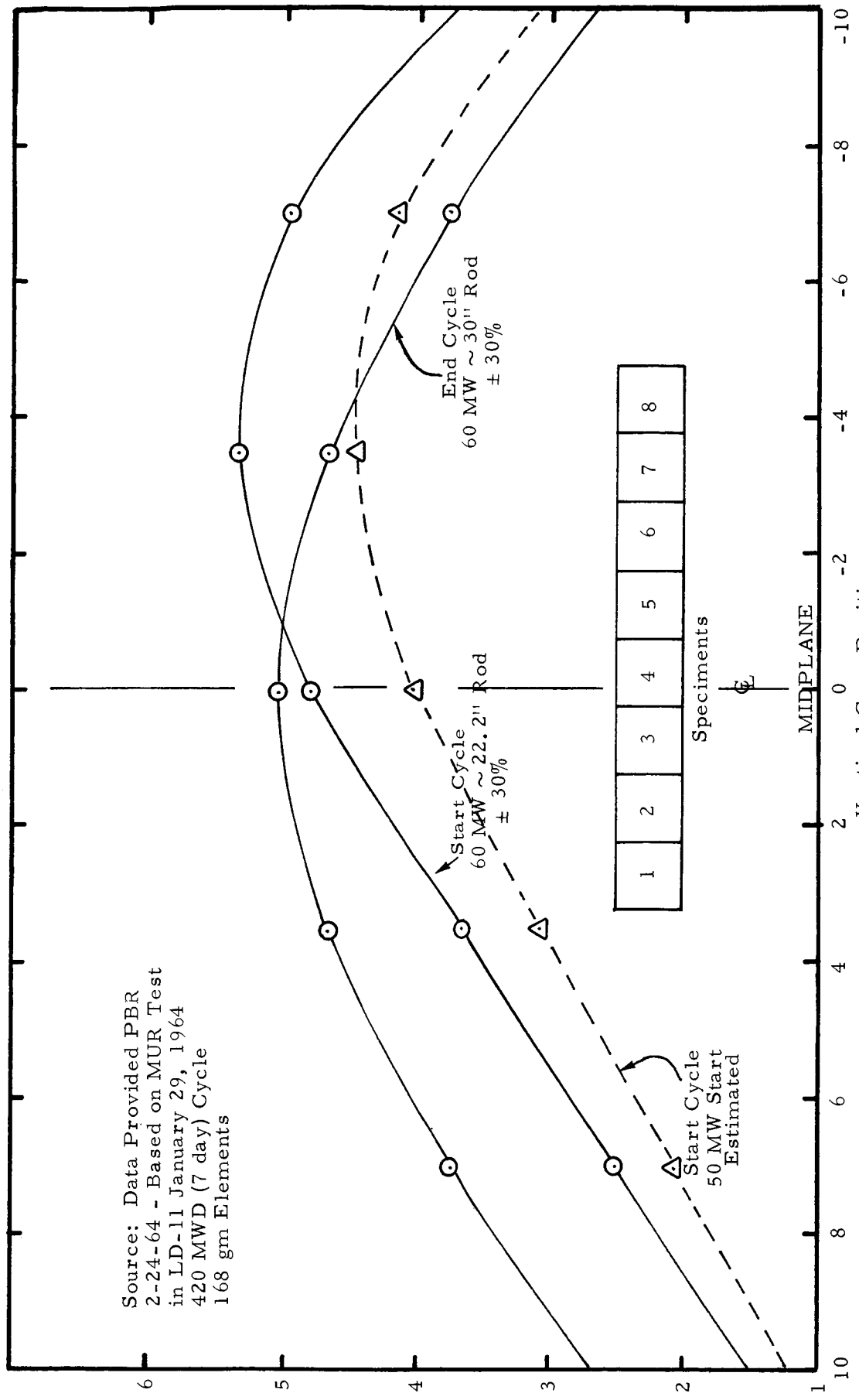

Figure 7. GAMMA HEAT VS VERTICAL CORE POSITION AND LOCATION OF SPECIMENS

1. Thermal Mock-Up of Capsule Sub-Assembly

A thermal mock-up was fabricated and tested in order to confirm the calculated tolerances that were determined by the thermal analysis of the capsule and the cold tolerances necessary for assembly as well as the mechanical and thermal integrity of the specimen electrode assembly. The capsule sub-assembly tested corresponded to the unit illustrated in Figure 5. This unit was completely instrumented and heated by radiation heat supplied by a tungsten filament and was tested in a vacuum environment. The unit was also used to measure the electrical resistivity of the Lucalox specimen. During the testing program, the sub-assembly was also subjected to a limited number of thermal cycles. Details of the experiment are presented in Appendix A.

Heat transfer calculations were performed using the test data obtained from the experiment and corroborated the results of the design analysis. After testing, the unit was disassembled and the Lucalox appeared in good condition, with the exception of three hairline cracks observed in the lower lip area; the cylindrical test area of the Lucalox was sound and crack free. No distortion or dimensional changes of the parts occurred; this satisfied the tolerance requirements. The only other design factor that remained to be evaluated was the electrical measurements and electrical contact resistance.

2. Electrical Measurements of Lucalox

During the thermal mock-up test of the Lucalox specimen electrode assembly, electrical resistivity measurements of the Lucalox specimen were performed. The data are plotted in Figure A. 1 of the appendix, along with published data of the resistivity of alumina measured in an air environment. Although the results, in general, are in agreement, the resistivity measured in a vacuum are somewhat higher particularly at higher temperatures. The details of the tests are covered in Appendix, Section A. 1.

In another test, a Lucalox specimen and the electrode assembly was used to measure the electrical resistivity (ohm-cm; Ω-cm) of the specimen under isothermal conditions in a vacuum environment. Measurements were made at 990°C, and the results of electrical resistivity compare favorably with published data on pure polycrystalline and single crystal alumina. The data and details of the test are presented in Appendix A.

During the design analysis, concern was expressed over the possible contact resistance masking the resistance of the specimen since a slip fit type design was used. Thermal expansion of the parts to make a solid contact at temperature was used instead of bonding. The problem reduces to showing that the contact resistance is much less than the specimen resistance at all experimental conditions for the proposed configuration. The design analysis showed that a resistivity minimum of 10^5 Ω-cm was expected for the specimen during the experiment. This corresponds to a specimen resistance minimum of about 6×10^3 Ω. Thus, it was necessary to have a contact resistance less than 6×10^3 Ω.

Information on useful values for the contact resistance experienced from metal-to-oxide pressure contacts were not available. Therefore, an experimental study was performed. The method used was to form pressure contacts between some metals and an oxide, impose a d-c potential across the couple, measure the resulting current, and map the potential drops with a potentiometer. In order to allow measurements to be taken at room temperature, a single-phase, semi-conducting oxide was substituted for the alumina insulator. The oxide used was $Nb_2O_{4.978}$; it was fully-dense and fine-grained. The resistivity of this oxide at room temperature was about 1 Ω-cm. Using various metals (Cu, Au, Pt, and Mo), the potential was mapped along the metal and the specimen. In addition, the potential drop across the stainless steel specimen interface was determined. The results are summarized in in Table II. R_c is the measured contact resistance. Over the pressure range

studied (10-50 psi) R_c was relatively unaffected by pressure. The contact area was approximately 1 cm^2. The applied pressure was a static (dead weight) load.

TABLE II

Contact Resistance

Interface	I (amps)	V (volts)	R_c (ohms/cm^2)
SS-Cu	0.041	0.00033	0.0083
Cu-Au-NB_2O_5	0.041	0.842	20.5
Nb_2O_5-SS	0.042	$6>\Delta V>1.5$	$143>R>35.7$
Cu-NB_2O_5	0.027	$6>\Delta V>1.5$	$222>R>55.5$
Cu-Pt	0.0375	0.0001	0.0026
Pt-Nb_2O_5	0.037	1.46	39.5
Mo-Nb_2O_5	0.023	~ 3	~ 130

The contact resistance between a polished oxide surface and a soft metal (e.g. Au) was about 20 Ω/cm^2 under 10 to 50 psi pressure. For a less ductile metal (e.g. Mo) the resistance was about 150 Ω/cm^2. It was clear that the contact resistance decreases with both increasing pressure and increasing temperature. Therefore, contact resistance should be negligible ($<<10^4$ ohms) in the in-pile experiment provided close dimensional tolerances and well-polished surfaces were maintained for both insulator and metal contacting parts in the operating temperature range of 800 to 1000°C.

E. Capsule Instrumentation and Console

1. Instrumentation

The Kovar inner electrodes were welded together to form a continuous common electrode and to aid in the assembly of the capsule. A nickel electrode measurement wire was welded to each of the molybdenum electrodes and the common center electrode. A nickel flux wire was inserted down the center hole of the Kovar inner electrodes. Four Inconel sheath Pt vs. Pt 13% Rh thermocouples which measured four of the inner electrode temperatures during operation were also included. The wires from the electrodes and the thermocouples were insulated with high purity alumina tubing and routed through the flutes of the stainless steel retainers. The entire assembly was contained in a stainless steel tube approximately 40 inches long so that the vacuum-tight electrical feed-through consisting of fifteen individual ceramic-to-metal seals was placed in a cool, low flux region. This was done to minimize effects due to the leakage resistance of the ceramic-to-metal seal and any changes due to radiation. A dummy electrical lead and thermocouple were placed in the seal so the leakage could be subtracted from the data taken for each specimen. The instrumentation leads and the thermocouple sheaths were brazed into the vacuum feed-through.

Immediately outside of the stainless steel vacuum can was an electrical heater used to provide fine temperature control of the capsule during irradiation. Surrounding the vacuum can was a containment can which provided the barrier between the capsule and the reactor cooling water. The region between the vacuum can and the containment can was filled with approximately 175 psig of helium, which provided the heat transfer medium from the vacuum can to the reactor coolant. All of the lead wires and thermocouple wires on the external side of the ceramic-to-metal feed-through were connected to the shielded instrumentation leads running from the experiment, through the pressure vessel, and to the experiment console.

2. Console

A console for experiment control and data acquisition was designed and assembled. A multi-point recorder was used for recording all temperatures as sensed by the thermocouples in the capsule. To measure the leakage current through the specimens, a Keithley electrometer was used. Power source for the experiment was provided by a d-c voltage from a Hewlett Packard regulated d-c power supply. The trim heaters in the capsule were powered by a variable transformer (Powerstat).

The voltage from the common center electrode to each individual outer electrode was supplied by the power supply through an appropriate selector switch to select the electrode for individual measurement. The currents from the instrumentation leads were measured with an electrometer circuit. The lead resistances were on the order of 10^6 ohms. The resistance of the ceramic-to-metal feed-through was extremely high, on the order of 10^5 higher than the specimen resistance at temperature.

F. Capsule Fabrication and Check Out

1. Capsule Assembly

All the capsule components were machined from material of known composition and that had satisfied the specifications and quality control inspection. All parts were chemically cleaned and prefired after machining. The capsule assembly was completed using clean room techniques that had been established for thermionic converters. The capsule parts, the alumina specimens, the electrodes, vacuum can and seal are shown in Figure 8. The partially assembled capsule consisting of the vacuum seal, specimens and leads

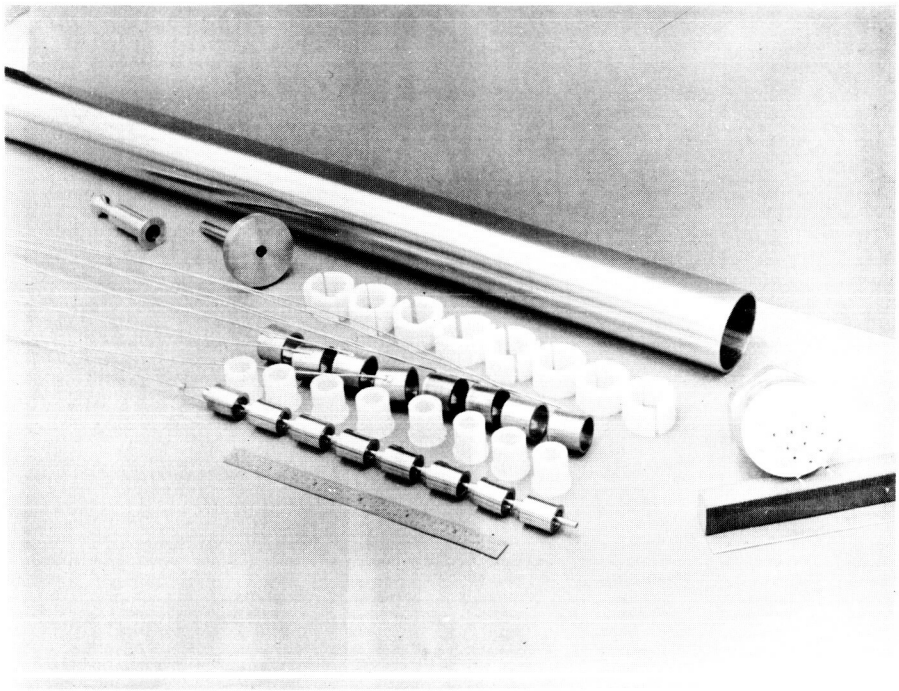

Figure 8. PARTS OF THE ALUMINA IRRADIATION CAPSULE SHOWING THE EIGHT ALUMINA SPECIMENS, ELECTRODES, VACUUM CAN AND SEAL PRIOR TO ASSEMBLY.

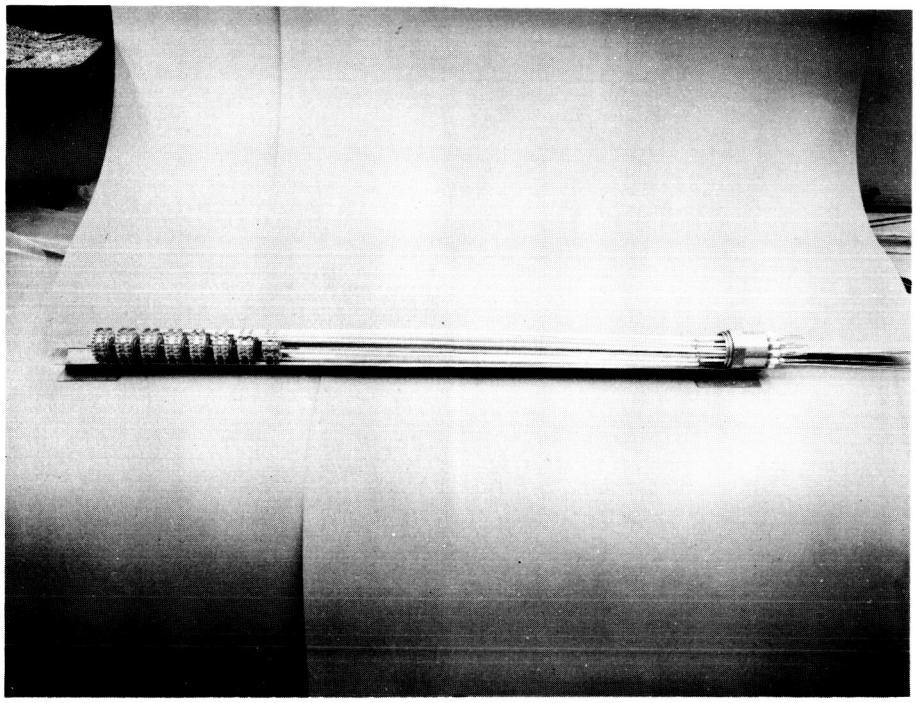

Figure 9. ALUMINA SPECIMENS, LEADS, AND VACUUM SEAL PRIOR TO INSTALLATION IN VACUUM CAN

is illustrated in Figure 9 prior to installation in the vacuum can. All of the electrical leads were insulated with high purity alumina sleeves. The capsule was installed in the vacuum can and pumped down on a vacuum station and heated to 675°F before the pinch-off. After cool down to room temperature, the pinch-off was performed with a vacuum of 8×10^{-6} torr.

2. Capsule Test

The capsule assembly was tested at the PBRF prior to installation in the reactor pressure vessel. The leads and thermocouples were checked and recorded. The capsule was then checked for core fit in the PBR Mock-up Reactor. The capsule, lead hose, and pressure vessel penetration were helium leak tested at 190 psig helium pressure. Two leaks were found in the penetration that had not been detected in final check of the capsule. These were repaired and the capsule passed the requirements with a helium leak rate of 10^{-6} cc/sec as measured with a mass spectrometer.

The capsule then was subjected to a hydraulic test. A pressure of 8 psig of helium was applied in the lead system with an outside water pressure of 65 psig. The water pressure was raised to 225 psig for two hours. The penetration flange, nut, and gasket performed satisfactorily. All leads were checked several times during the test. The pressures were adjusted to 182 psig helium and 149 psig water and held for 20 hours. The helium pressure held to within two psi and this test was considered satisfactory.

The capsule was removed from the hydraulic test and helium leak checked to 190 psig. The leak rate was 10^{-3} to 10^{-4} cc/sec. This leak was traced to the MgO insulation on the leads at the pressure vessel penetration. Since this would only result in a helium loss of approximately 1 ft^3 per cycle, the test was considered satisfactory.

During these tests, the lead to the common resistances dropped below the megohm range on several leads. This was apparently due to moisture pick up in the MgO insulation of the leads at the pressure vessel penetration. The leads were baked out and the resistances restored to the 10^6 ohm level. The MgO was sealed with Glyptal and RTV silicone sealant. It was also found that the lead resistance was a function of whether the helium pressure was applied to the system or not. When the lead system was depressurized, the lead to common resistance tended to go down. This is believed to be due to moisture pick up in the MgO insulation from the humid atmosphere near the pressure vessel penetration. When the lead system was repressurized, the resistances returned to values in the range before depressurization.

Due to the use of metal sheath electrode leads and metal thermocouple connectors in accordance with PBRF requirements, it was impractical to prevent common lead grounding. As a result, a wiring modification was made at the console to use ground and a common lead and float the power supply.

In order to remove the capsule from the PBR, a special remote cutoff shear was required. The cutoff shear tool was tested and shipped to the PBRF.

G. Hazards Analysis

1. Hazards Considerations

The hazards analysis for this experiment was performed in accordance with the "Information for Experiment Sponsors for the NASA Plum Brook Reactor Facility, Parts I, II and III." This experiment was inherently one which involved a low hazard in that it did not contain fissionable fuel material or finely divided materials that could result in high-energy, long-lived isotopes when activated, and it was heated primarily

by gamma heat. The specimens were doubly contained in stainless steel cans. The inner can contained the specimens in a vacuum. The vacuum can was protected by a helium atmosphere which was captive and not vented to the outside of the reactor pressure vessel by gas lines. The outer containment was pressure tested to over 1-1/2 times the anticipated maximum operating pressure. The experiment was failsafe with respect to the maximum credible accident, to be discussed later. The only leadout for this system was electrical.

The only condition that could arise in the capsule that would require a reactor power reduction would be over temperature indication of the specimens or vacuum can.

2. Maximum Credible Accident

The maximum credible accident would be overheating of the specimens or vacuum can. Three cases were analyzed which could conceivably lead to a high temperature condition. This condition, of course, was the accident of most concern.

Possibilities considered in light of the maximum credible accident were steady-state operation at 150% reactor power at maximum reactor and trim heater power with no coolant flow. Additional conditions were considered; i.e., loss of system coolant flow and pressure, system rupture, loss of electrical power, reactor excursion, boiling, handling accidents, instrument failures, control system failures, chemical reactions, effect of flooding or voiding, damage to the lead system and leakage of primary water or gas to the containment vessel.

In all cases, the analysis indicated a very low probability of a hazardous situation.

H. In-Pile Electrical Measurements

During the course of the irradiation, measurements were made of electrical resistivity and breakdown voltage of the Lucalox alumina. A voltage of 100 V dc was applied to each alumina insulator by a fused selector switch. The current was measured by an electrometer (10^{-3} to 10^{-12} amps) at the console. The d-c voltage was applied by an adjustable regulated power supply. The resistance was calculated from the d-c voltage and the current. The seal temperature and the resistance were read using the seal dummy connection and thermocouple each time. The seal resistance was very large compared to the specimen resistance. The resistance, R, was computed from the two resistances in parallel by the following relation:

$$R = (R_{seal} X R_{specimen})/(R_{seal} + R_{specimen}).$$

In general $R \cong R_{specimen}$

For cylindrical specimens, the resistivity

$$\rho = 2\pi L R_{specimen}/\ln(r_3/r_2)$$

where ρ = resistivity, L = length, and r_2 and r_3 are the radii. A megohm meter was also provided for measuring resistance.

At the end of each irradiation cycle, 300 V dc was applied to each Lucalox specimen to check the breakdown. If a breakdown occurred, the fuse at the selector switch would blow and eliminate that specimen from the experiment. The in-pile data were analyzed on the basis of the electrical circuit diagram shown in Figure 10. On the right is the schematic network

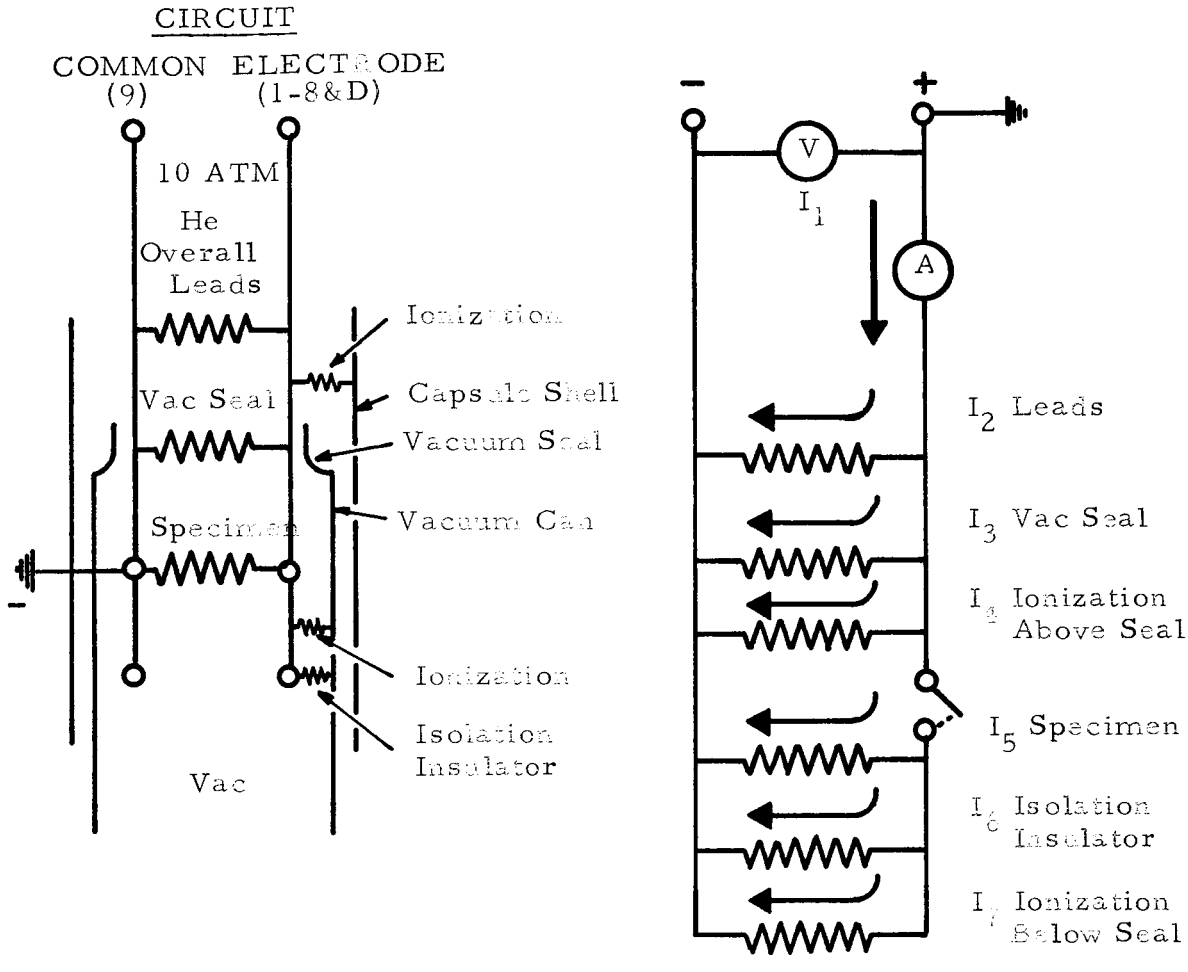

Figure 10. IN-PILE MEASUREMENT CIRCUIT DIAGRAM

used in the analysis of the data. The various equations used in the analysis are presented in Table III.

TABLE III

Equations Used In Data Analysis

$I_1 = I_2 + I_3 + I_4 + I_5 + I_6 + I_7$

I_1 = measured current for specimen

$I_2 + I_3 + I_4 = I_8$ or total lead system plus leakages

I_8 = measured current for lead leakages (dummy)

$R_{spec} \times 11 = R_{isolation\ resistor}$

$$\frac{V}{I_{spec}} \times 11 = \frac{V}{I_{isolation\ current}}$$

$I_{spec} = 11\ I_{isolation}$ or $I_5 = 11\ I_6$

$I_4 >>> I_7$

$I_1 - I_8 \approx I_5 + I_6$ or $I_1 - I_8 = 1.091\ I_5$

$$I_5 \approx \frac{I_1 - I_8}{1.091}$$

$$R = \frac{\rho \ln \frac{r_2}{r_1}}{2 \pi L}$$

$$\rho = 91.9 \frac{V}{I_5}$$

$$\rho = 100.2 \frac{V}{I_1 - I_8}$$

I = current, amps

R = resistance, ohms

ρ = resistivity, ohm-cm

V = applied voltage

EXPERIMENTAL RESULTS AND DISCUSSION

A. In-pile Electrical Measurements of Lucalox Alumina

In measuring the electrical properties of the alumina a current resulted from the ionization of the helium atmosphere due to the high nuclear radiation flux above the ceramic-to-metal seal. This flux caused a great number of ion pairs to be generated in the helium atmosphere and ionization currents non-symmetric with respect to polarity were observed. The polarity definition in this case was defined as the center electrode positive and the outer individual electrodes being negative. This center electrode was grounded to the vacuum can and containment can wall because of the sheath grounded mineral insulated lead-out wires. In the positive polarity case, very low ionization currents were observed. This was due to the ion mobility being the determining mechanism for current flow and the fact that the effective collection volume was only that amount of nickel electrode wire protruding past the ceramic insulation above the ceramic-to-metal seal. Where the polarity was reversed, and the vacuum can was negative with its extremely large effective collection volume, the large ionization currents were observed. Therefore, only positive quadrant data were used in the measurement of the in-pile resistivity. These effects were measured once each time the data for all eight specimens were obtained by measuring the observed currents in a dummy electrode lead that led down through the vacuum ceramic-to-metal seal but did not extend down to an electrode. In this manner, the current value for the leads, the leakage resistance of the vacuum seal and the ionization currents were measured. The specimen current was calculated from the relation shown in Table III. The current leakage through the isolation insulator was small when compared to the specimen current because its thickness was much larger and it was at a lower temperature than the specimen. Ionization within the vacuum can was assumed to be negligible in the data reduction. The effect of this is considered later in the discussions of the post-irradiation examination.

Electrical resistivity measurements were made at discreet periods of time during each reactor cycle. In between these periods, 100 volts were applied to specimen No. 3 on a continuous basis. During each reactor cycle, or about once each 170 hours, 300 volts were applied sequentially to each of the eight Lucalox specimens.

The data recorded on specimen Nos. 6 and 8 are plotted in the form of log resistivity in ohm centimeters vs. specimen temperature in Figures 11 and 12 respectively. These specimens were selected for the data plots because a thermocouple was located on the inner electrode, thus reducing the temperature uncertainty. The specimen temperatures varied because of the gamma flux distribution shift associated with normal fuel burnup of the reactor core. The temperature profile during one cycle of the PBR is plotted in Figure 13. The out-of-pile measurements made on an identical alumina (Lucalox) specimen are shown by the solid line, whereas, the actual in-pile data points are shown as circles. From these figures it is evident that the integrated neutron dose up to a total dose of 1.6×10^{20} >1 Mev had very little effect on electrical resistivity of the Lucalox specimens. The total fast neutron dose for this experiment ranged from approximately 1.4 to 1.6×10^{20} nvt. The calculated neutron exposure as a function of time in the reactor is shown in Figure 14. The analysis from the nickel flux wire is also presented. From Figures 11 and 12 it is also observed that the absolute value c electrical resistivity appears to be approximately a factor of five (5) higher than the out-of-pile data. These results were typical of the other Lucalox specimens; the data for each specimen are presented in Appendix B.

At a dose of approximately 1×10^{20} nvt, a 1/8 amp fuse in series with the electrode measurement line failed at 270 volts indicating possible breakdown of specimen No. 3. Subsequent attempts produced the same result at approximately 270 volts. However, subsequent resistivity measurements made on that specimen showed no change from the values obtained prior to the first fuse failure. This is further discussed in the post-irradiation section of the report. None of the other five specimens showed signs of

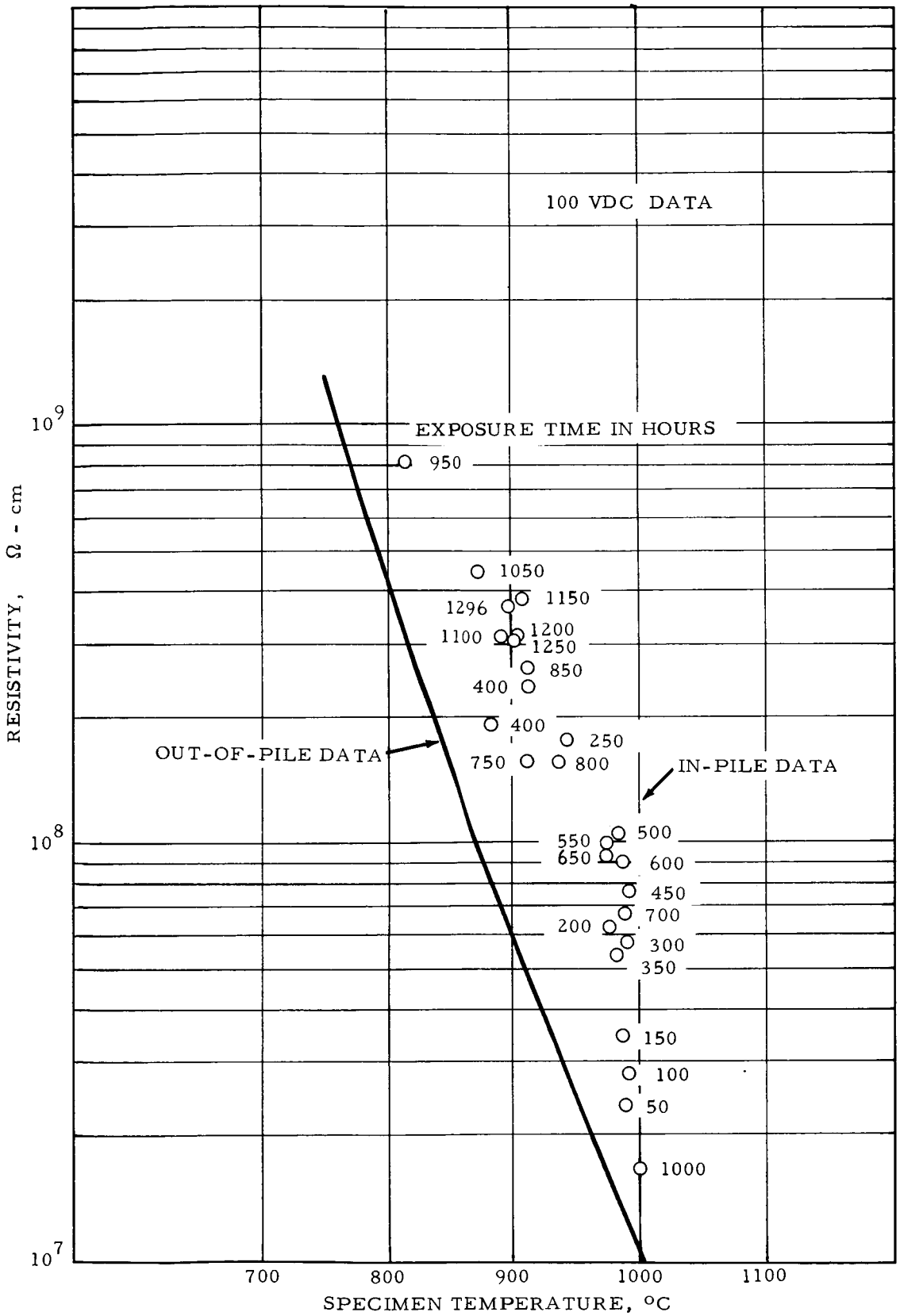

Figure 11. RESISTIVITY vs TEMPERATURE FOR VARIOUS EXPOSURES - SPECIMEN No. 6

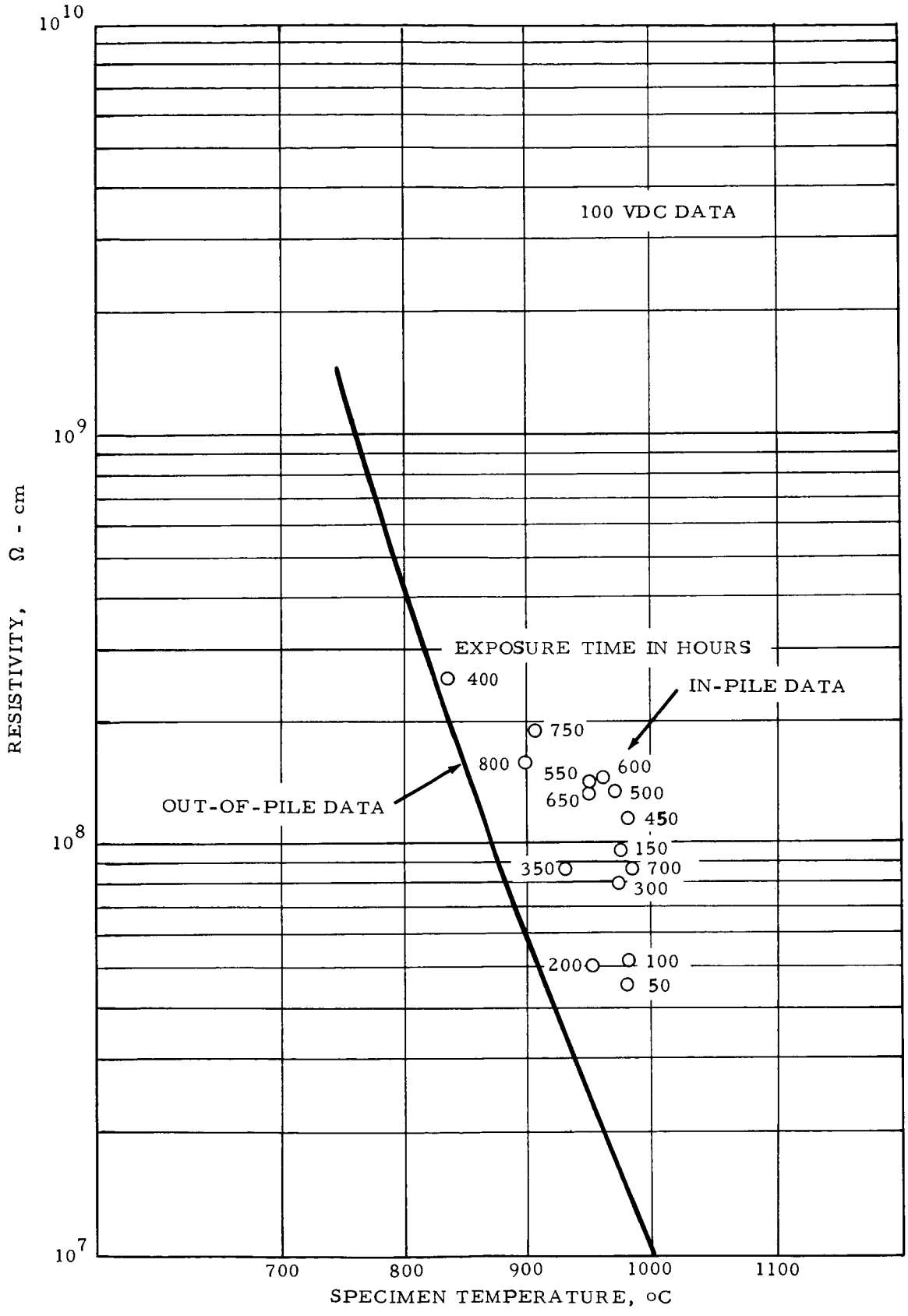

Figure 12. RESISTIVITY vs TEMPERATURE FOR VARIOUS EXPOSURES - SPECIMEN No. 8

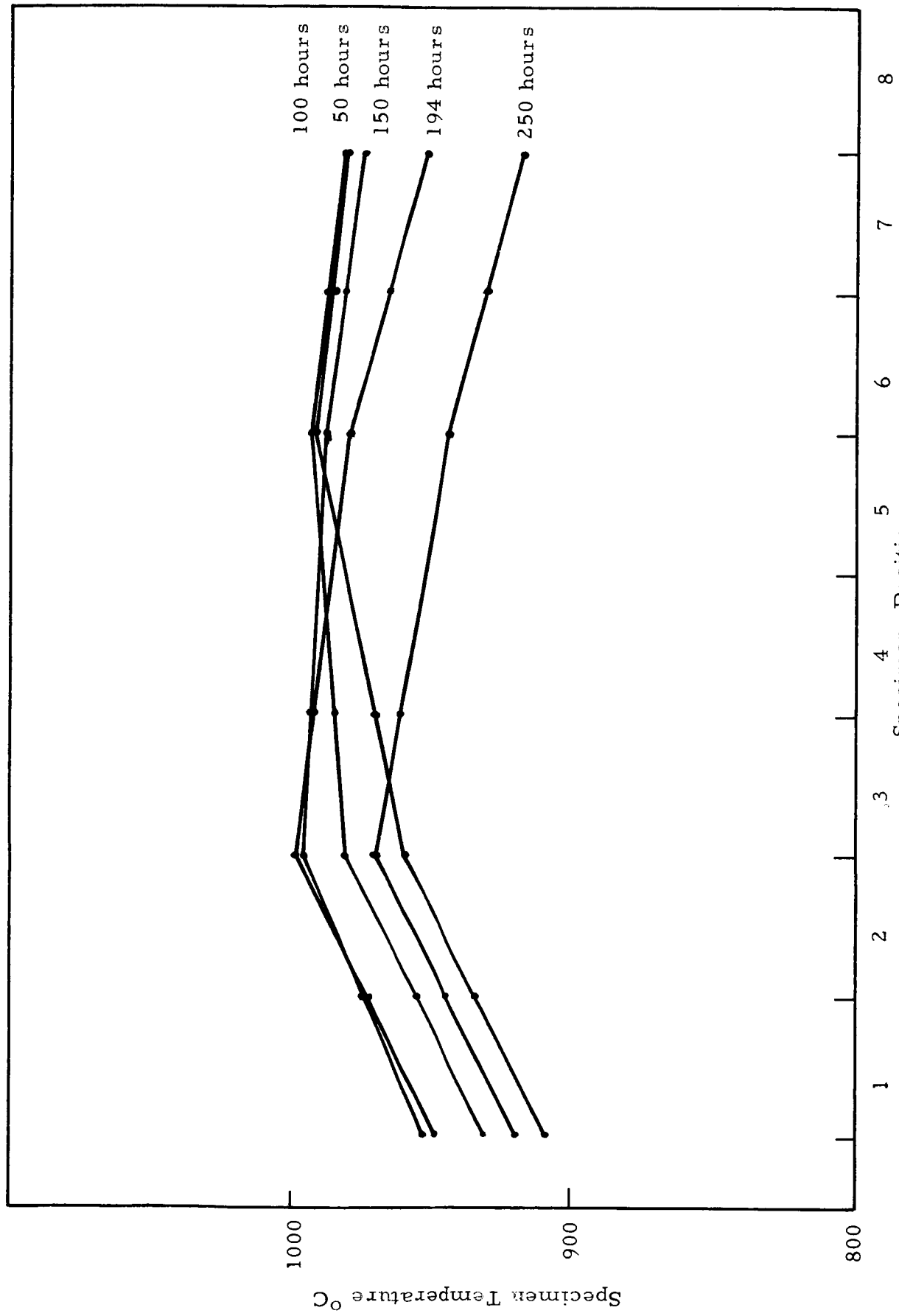

Figure 13. ALUMINA IRRADIATION SPECIMEN TEMPERATURE PROFILES DURING PBR CYCLE NO. 23

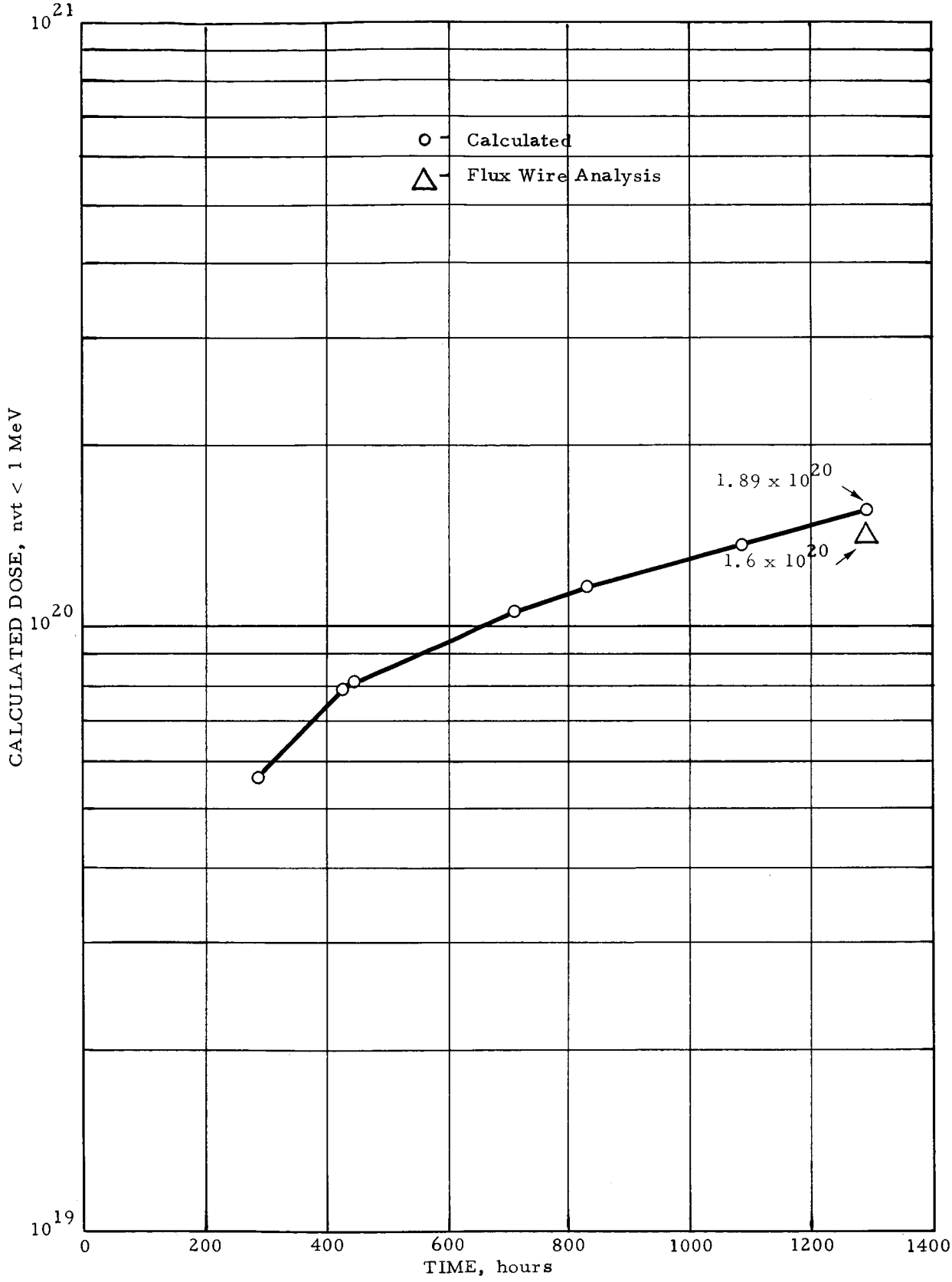

Figure 14. NEUTRON EXPOSURE (nvt) > 1 MeV vs TIME IN REACTOR

possible breakdown during the test. The total exposure was 1290 hours at which time the experiment was removed from the Plum Brook Reactor and the specimens within the vacuum can were shipped to the General Electric Vallecitos Nuclear Center for post-irradiation examination.

B. Post-Irradiation Examination of Capsule

The capsule examination was performed in the Radiation Materials Laboratory (RML). The external surfaces of the capsule were visually examined, and the entire assembly appeared to be in good condition. The aluminum sleeves covering the upper part of the capsule were removed. Inspection of the inside surfaces of the sleeves and exposed capsule surface showed only minor white surface discolorations, which were determined to be water stains from storage.

1. Internal Gas Pressure Measurement and Analysis

A vacuum seal was made between the outer surface of the upper capsule wall and the standard RML puncture device. After evacuating the entire vacuum system to a pressure of 2×10^{-4} torr, and establishing a system pressure drop rate of 1.5×10^{-4} torr/min., a sharpened steel pin was driven through the wall of the capsule by means of a hydraulic ram. The pressure of the system equilibrated at 5.3 torr. This value, plus the known system volume and estimated internal capsule volume of 540 cm^3 permitted the capsule pressure at the time of puncture and the amount of gas present to be calculated. A total gas sample of 6.57 cm^3 (STP) was collected.

Six aliquots of gas from the bottle were analyzed by gas chromatography. The percentages detected after correcting for residual argon in the sampling system were:

Gas	Vol. %
H_2	94.3
He	4.22
N_2	1.24
O_2	< 0.25

The relatively large amount of H_2 present was believed to have originated from some of the internal capsule parts (i.e., Kovar) which were hydrogen-fired prior to capsule assembly. The amount of helium present seems to be consistent with the amount expected to leak in from the external gas coolant during irradiation (based on a leak rate established by pre-irradiation helium mass spectrometer leak tests). The small amounts of N_2 and O_2 probably resulted from some air leakage into the system during the puncturing and sampling operation.

2. Visual Examination of Sample Assembly

The capsule assembly was dissected to permit evaluation of all the irradiated Lucalox specimens. The capsule sleeve was removed with a series of transverse and circumferental cuts to minimize disturbance of the specimens prior to observation. Removal of one-half of the sleeve then exposed the entire sample assembly.

With a minimum of disturbance, the specimen assembly and inside surface of the capsule wall were carefully examined and the assembly appeared to be in good general condition. All of the Lucalox samples were found to have turned from white to a dark gray color. The alumina isolation blocks were also darkened, but not to the same degree as the Lucalox specimens. The only evidence of specimen breakage observed at this time was the slight cocking of the upper end of Specimen No. 8.

Surface impressions of the teeth of the outer stainless steel spacers were quite pronounced in each sample location, indicating good contact during irradiation. A discolored region (primarily surface interference colors) on the inside surface of the vacuum can was limited to the upper two inches of sample No. 1. Below this level a surface deposit was observed which became increasingly heavy toward the bottom end, with a maximum concentration about three inches above the bottom sample (No. 8). The deposit was a light gray-tan in color and was found to be very loosely adhered to the surface. A sample was scraped off with a clean wooden spatula and submitted for X-ray analysis. One sample was analyzed by the powder diffraction technique and the major constituent was initially identified as molybdenum, with trace amount of stainless steel, and possibly a very small amount of Al_2O_3. However, subsequent X-ray fluorescence analysis of a second sample showed the major element to be manganese, with minor and trace amounts of iron, nickel, copper, chromium, and cobalt. This analysis revealed no evidence of molybdenum. Further analysis of the original powder diffraction pattern showed that the lines originally identified as molybdenum were actually those of manganese-oxygen, which has a structure similar to that of molybdenum.

3. Sample Disassembly and Visual Examination

The nickel flux wire was removed from the assembly and stored in a special tube for subsequent gamma scanning and sampling. The entire specimen assembly was then completely removed from the capsule tube half. The Lucalox samples were individually removed from their sub-assemblies by cutting through the Kovar pin connecting two assemblies, and then removing the Lucalox specimen and inner Kovar electrode from the outer molybdenum electrode. Each of the specimens were carefully examined and photographed. Photographs of the specimens during post-irradiation are shown in Figure 15.

Specimen No. 1 with Kovar Electrode in Place

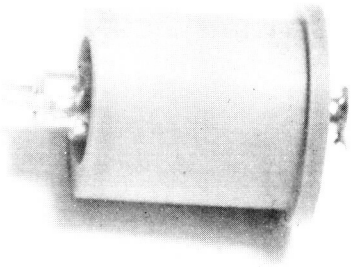

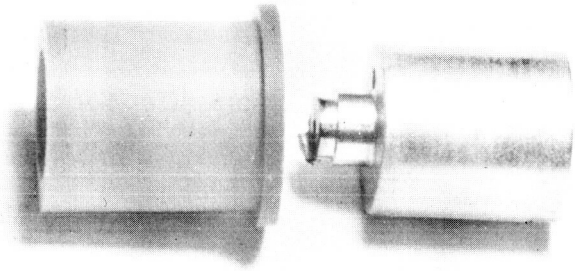

Specimen No. 2 with Kovar Electrode Removal

Specimen No. 3 with Kovar Electrode Removed

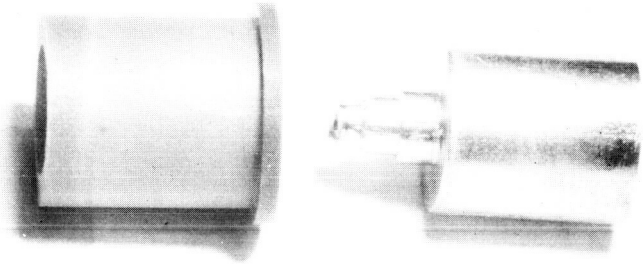

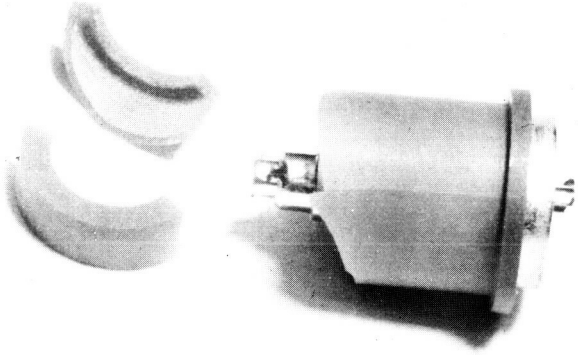

Specimen No. 4 with Kovar Electrode in Place, showing Circumferential Fracture Near the Lower Lip

Figure 15. PHOTOGRAPHS OF SPECIMENS DURING POST-IRRADIATION EXAMINATION

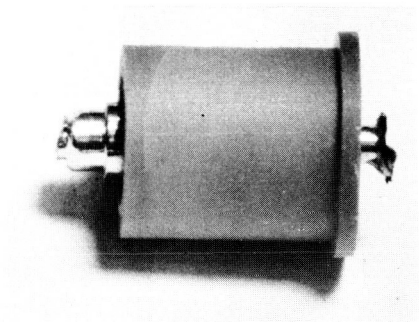

Specimen No. 5 with Kovar Electrode in Place

Inside Surface of Specimen No. 6 as Held by Manipulator Fingers, Showing Deposit

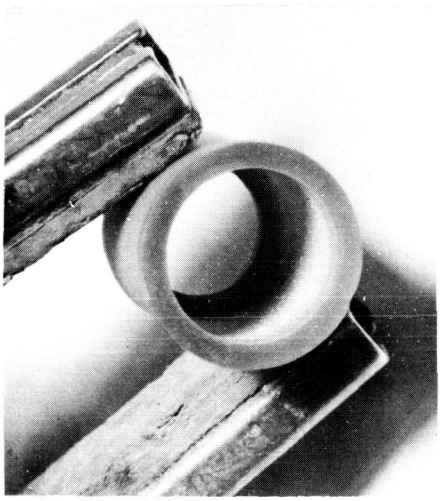

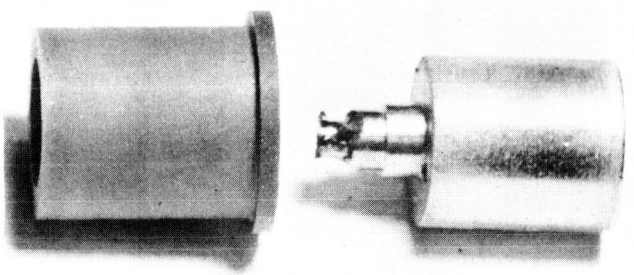

Specimen No. 7 with Kovar Electrode Removed

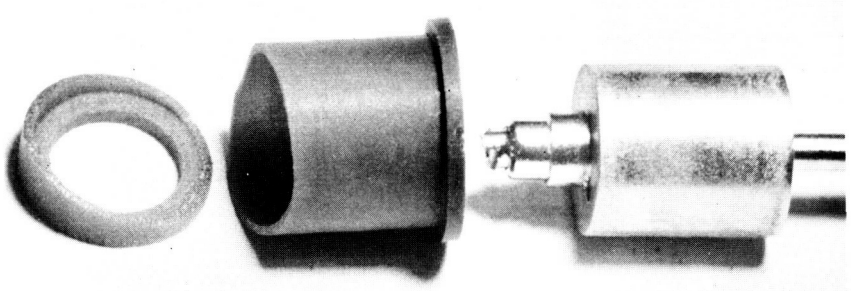

Specimen No. 8 with Kovar Electrode Removed; Note Circumferential Fracture at Lower Lip

Figure 15. PHOTOGRAPHS OF SPECIMENS DURING POST-IRRADIATION EXAMINATION

Three of the specimens adhered to their Kovar electrodes. No specimens were bonded to the molybdenum electrodes. All of the specimens had become darkened (Figure 15). Variation in the degree of darkening was noted, with the upper specimen Nos. 1 and 2 being light to medium gray, and the lower specimens being dark gray with No. 8 approaching black. Visual examination of the inside surfaces of all those specimens which were not stuck revealed light, almost metallic appearing deposits. These deposits were not identified and no attempts were made to obtain specimens for analysis. However, radioactivity measurements of two specimens (Nos. 6 and 7) revealed dose rates of 4 to 5 rad/h at a distance of 12 inches. These unexpectedly high activity levels was probably due to cobalt-60 contamination from the Kovar.

Some of the specimens cracked circumferentially and fractured as shown in Figure 15. The pertinent features of each sample are summarized in Table IV.

TABLE IV

Post-Irradiation Examination of Specimens

Specimen No.	Observations
1	Stuck to Kovar electrode. No cracks, very small chips broken out of edge of inner flange.
2	Not adhered to Kovar electrode, no cracks, light deposits inside surface.
3	Not stuck to Kovar, no cracks, light deposits inside surface. (No indication of electrical breakdown).
4	Partially stuck to Kovar electrode, two pieces of inner flange section fractured circumferentially detached from electrode, light deposits on exposed inside surfaces. Darkening through entire cross-section of exposed

TABLE IV - (Continued)

4 (continued)	fracture surfaces, one longitudinal fracture through entire length of section still stuck to electrode.
5	Stuck to Kovar electrode, circumferential crack immediately adjacent inner flange. Sample still intact.
6	Not stuck to Kovar, no cracks, light deposits inside surface.
7	Not stuck to Kovar, no cracks, light deposit inside surface.
8	Not stuck to Kovar, complete circumferential fracture at inner flange end, flange section broken off as complete ring, entire exposed cross-section darkened, light deposits inside surface.

It is not definitely known what caused the observed fractures, although it is quite possible that they occurred during the disassembly operations. The only indication of a fracture observed prior to the final disassembly was the slightly cocked inner flange end of sample No. 8 previously mentioned. Examination of the Kovar electrodes which were not stuck showed them to be clean and in good condition. There was no obvious evidence of surface reactions.

The outer assembly of sample No. 4 was taken apart to completely expose the molybdenum electrode. With the exception of some slight discoloration in the inside surface, this electrode appeared clean and in good condition. The remaining parts of this subassembly all appeared to be in good condition. None of the four alumina blocks were damaged, although they had developed a light gray discoloration, as previously mentioned. The

outer fins of the stainless steel spacers were covered with the same type of deposit observed on the inside surfaces of the capsule tube, and the inside surfaces appeared to have developed some variations in texture which appeared to be related to the position of the alumina blocks.

4. Dimensional Measurements

The outside diameters and lengths of all but the broken Lucalox specimens were measured remotely to the nearest one-half mil with a micrometer. These data are compared to the original specimen dimensions in Table V. From these data, it is evident that no significant dimensional changes occurred in the Lucalox as a result of the irradiation.

TABLE V

Lucalox Sample Dimensions

Specimen No.	Post-Irradiation Diameter		Pre-Irradiation Diameter		Post-Irradiation Length		Pre-Irradiation Length	
	0°	90°	0°	90°	0°	90°	0°	90°
1	0.626	0.626	0.6260	0.6260	0.752	0.752	0.7510	0.7510
2	0.626	0.626	0.6260	0.6260	0.754	0.752	0.7520	0.7515
3	0.626	0.626	0.6255	0.6252	0.754	0.754	0.7550	0.7545
4	0.626	0.626	0.6260	0.6260	- - broken - -		0.7505	0.7500
5*	0.627	0.627	0.627	0.6255	0.735	0.754	0.7540	0.7540
6	0.626	0.626	0.6252	0.6252	0.754	0.753	0.7540	0.7540
7	0.626	0.626	0.6255	0.6255	0.752	0.752	0.7515	0.7520
8	0.626	0.627	0.6255	0.6255	- - broken - -			

*Circumferentially cracked

The outside diameters of three Kovar and one molybdenum electrodes and the inside diameters of three molybdenum electrodes were also measured to the nearest one-half mil with micrometers and are presented in Table VI. On the basis of these data, the electrodes did not experience significant

deformation during the irradiation.

TABLE VI

Kovar and Molybdenum Electrode Dimensions

	Post-Irradiation outside diameter		Pre-Irradiation outside diameter		Post-Irradiation inside diameter		Pre-Irradiation inside diameter	
Sample	0°	90°	0°	90°	0°	90°	0°	90°
Kovar #2	0.559	0.559	0.5583	0.5584	- -	- -	- -	- -
Kovar #6	0.559	0.559	0.5585	0.5585	- -	- -	- -	- -
Kovar #8	0.559	0.559	0.5584	0.5584	- -	- -	- -	- -
Mo #1	- -	- -	- -	- -	0.629	0.630	0.6295	0.6295
Mo #4	0.741	0.742	- -	- -	0.629	0.628	0.6295	0.6293
Mo #8	- -	- -	- -	- -	0.630	0.629	0.6290	0.6290

5. Metallographic Examination

The Lucalox specimen No. 1, together with its attached Kovar electrode, was prepared for metallographic examination. The sample was potted in epoxy resin and ground in plane transverse to the longitudinal axis of the sample. Grinding was started at the inner flange end, and was continued until the flange lip was passed and a plane including the Lucalox-Kovar circumferential interface was reached. Examination of the specimen was performed under bright field and polarized light illumination. The microstructure of the Lucalox shown in Figure 16 was essentially the same as the pre-irradiated material. Examination of the interface revealed a region of very close contact between the Lucalox and Kovar which comprised about one-third of the circumference. Within this region a discontinuous band, approximately one-half mil thick, was observed at the interface (Figure 17). The band was more characteristic of the Lucalox, but was in intimate contact with both the Lucalox and Kovar. Whether or not this band represents a true

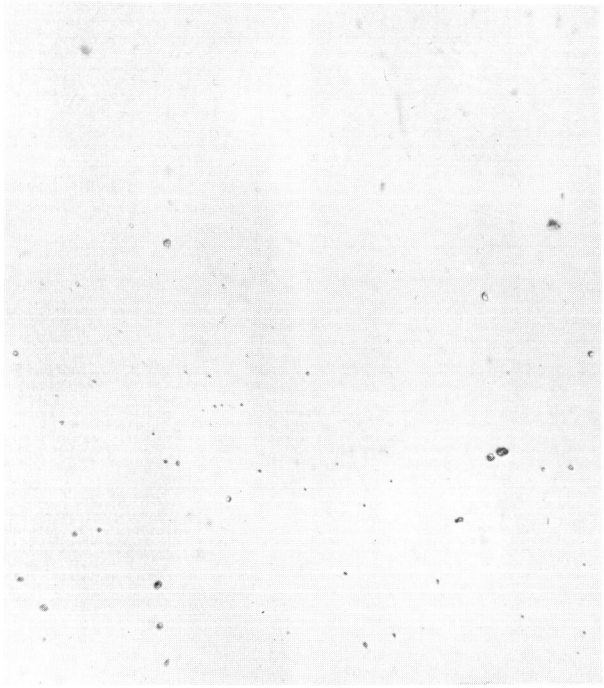

AS-POLISHED 250X

Figure 16. SECTION OF TYPICAL SPECIMEN SHOWING POROSITY UNCHANGED DUE TO IRRADIATION

KOVAR

LUCALOX

AS-POLISHED POLARIZED LIGHT 250X

Figure 17. PHOTOMICROGRAPH OF LUCALOX-KOVAR INTERFACE SHOWING REACTION ZONE - TYPICAL OF SPECIMENS STUCK TO KOVAR ELECTRODE

reaction zone could not be positively ascertained at that time. No evidence of reaction was observed over the remaining two-thirds of the interface.

6. Flux Wire Scan and Analysis

Pure nickel wire mounted axially on the capsule during the irradiation was gamma scanned and the readout plotted on a one-to-one length ratio chart trace to provide direct correlation between activity profile and assembly drawings. The shape of the gross activity profile, Figure 18, appeared to follow that of the axial neutron flux profile of the Plum Brook Reactor at the position in which this experiment was located. However, there were six very pronounced peaks and two lesser peaks superimposed on the general profile. The spacing between these peaks closely corresponded to the specimen spacings. The ratio of the maximum peak activity to that at its base was about 4, which is much too high to attribute to flux depression variations resulting from variations in the amount of hardware surrounding the wire. Four 1/4-inch long sections were cut from the wire at accurately measured locations. One section was taken from the maximum peak location and the other three from locations representing "valleys", for the overall acitivity levels of the wire.

Absolute fast flux determinations based upon the nickel-58 (n, p) cobalt-58 reaction were performed by radiochemical analysis. Determination of the fast flux values was found to be complicated by contamination of the wire with cobalt-60, the analysis of which is normally used to correct for thermal neutron burnup of cobalt-58 (cobalt-59 was present in nickel in small amounts, and was converted to cobalt-60). It was found that the section from the maximum peak was considerably more contaminated with cobalt-60 than the others, which leads to the conclusion that this contamination resulted from direct contact of the nickel wire with the Kovar parts, particularly in the narrow top end plug region of the Kovar electrodes.

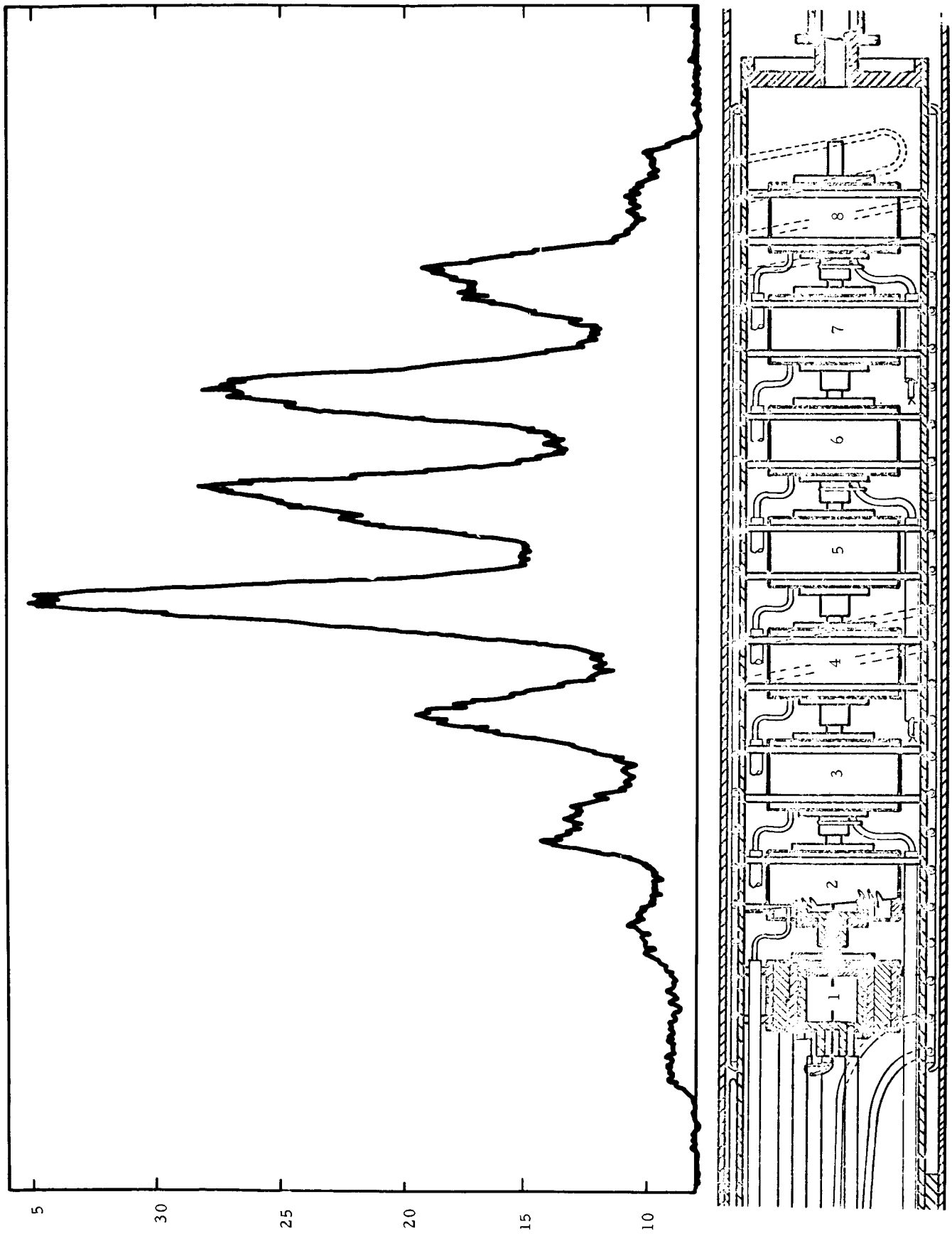

FIGURE 18 GAMMA ACTIVITY PROFILE

The fast flux exposures >1 MeV were evaluated from four nickel samples cut from the flux wire taken from the capsule using a computer code for fast flux calculations from irradiated nickel. Results appear in Table VII. The program accounts for thermal neutron burnout during multi-cycle reactor operations. The overall thermal neutron burnout correction for the Co-58 isomers for theoretical thermal fluxes was calculated to be 1.78.

Constants used in the calculations were:

Decay constant for Co-58m		1.848	$days^{-1}$
Decay constant for Co-58		0.00976	$days^{-1}$
Cross-section for the Ni-58 (n, p) Co-58m reaction	=	0.033	barns
Cross-section for the Ni-58 (n, p) Co-58 reaction	=	0.064	barns
Cross-section for the Co-58m (n, γ) Co-59 reaction	=	1.7×10^5	barns
Cross-section for the Co-58 (n, γ) Co-59 reaction	=	1650.0	barns
Fraction of neutron spectra above 1 MeV	=	0.692	
Ni-58 abundance	=	0.679	

TABLE VII

Fast Flux Exposures >1 MeV
Radiochemical Analysis of Ni Flux Wires

Sample	dps Co-58 / gm Ni @ 4-15-65	ϕ @ 100 MW Power	ϕ>1 MeV
1	2.00×10^9	9.7×10^{13}	1.6×10^{20}
2	2.05×10^9	9.9×10^{13}	1.6×10^{20}
3	1.99×10^9	9.6×10^{13}	1.6×10^{20}
4	1.76×10^9	8.5×10^{13}	1.4×10^{20}

A summary of the flux history for the irradiation is presented in Table VIII; the values were estimated from reactor operation data by the PBR Nuclear Analysis Section. This was not corrected for perturbing influences of surrounding hardware. The PBR estimated values compare favorably to the radiochemical analysis values of fast neutron fluxes.

TABLE VIII

Summary of Flux History for Experiment

Cycle	MWD	ϕ fast ϕ >1 MeV	ϕ fast/ϕ_{th}	Fast neutron dose (>1 MeV) nvt	Uncertainty at 95% Confidence	Position
23	448.7	0.64×10^{14}	0.20	0.63×10^{20}	±75%	LD-11
24	314.2	0.41×10^{14}	0.27	0.18×10^{20}	±50%	LA-11
25	53.4	0.34×10^{14}	0.27	0.026×10^{20}	±20%	LA-11
26	636.1	0.40×10^{14}	0.18	0.37×10^{20}	±35%	LA-11
27	253.8	0.42×10^{14}	0.13	0.19×10^{20}	±20%	LA-11
28	512.5	0.34×10^{14}	0.27	0.25×10^{20}	±20%	LA-11
29	505.0	0.34×10^{14}	0.27	0.25×10^{20}	±20%	LA-11
Total	2723.7			1.89×10^{20}		

APPENDIX A

OUT-OF-PILE TEST ON ALUMINA SPECIMENS

APPENDIX A

OUT-OF-PILE TEST ON ALUMINA SPECIMENS

Thermal Mock-Up Test of Capsule Sub-Assembly

In order to confirm the thermal design calculations, the dimensional tolerances that were dictated by the thermal expansion characteristics of the materials and to determine the ease of assembly, a special out-of-pile capsule specimen holder sub-assembly (Figure 5) was designed, fabricated and tested.

The test unit consisted of a single specimen sub-assembly, a 1-1/2 inch section of the vacuum can and heater wire which surrounded the can to simulate the actual capsule design. This unit was instrumented to measure the temperatures of the Kovar and molybdenum electrodes, the fin and the inside wall of the vacuum can. Also, electrical leads were placed on the Kovar molybdenum electrodes to permit measurements of the alumina resistance. Electrical measurements were made with the electrometer that was to be used in the capsule console.

The instrumented mock-up was suspended in a vacuum bell jar as shown in Figure A.1. A tungsten filament assembly was used to heat the inside of the Kovar electrode by radiant heating. After the bell jar was pumped down, a small amount of power was applied to the filament to bring the Kovar to a temperature of 400°C and the unit was then outgased overnight. The vacuum achieved during the test program ranged from 10^{-5} to 10^{-6} torr.

This mock-up simulated the actual capsule only in part since the source of heat in the capsule was the gamma heating of each part. In this test the radiant heat received at the inner Kovar surface was transferred out radially with no internal generation. The heat transferred from the outside surface of the vacuum can in the capsule was by radiation and conduction across a helium gas gap to the outer capsule wall and thus to a water heat sink. In this mock-up the heat was transferred from the vacuum can section by radiation to the bell

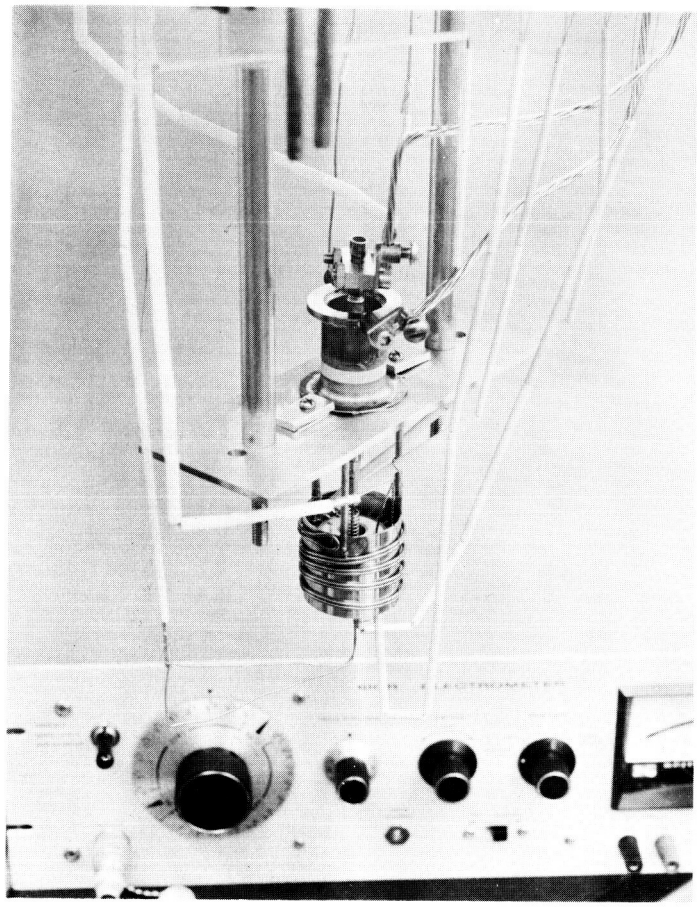

Figure A.1. TEST ASSEMBLY

jar wall only. A conduction correction factor was applied to obtain the simulated vacuum can and fin wall temperature. As was expected, the results of the mock-up test showed a higher uncorrected vacuum can wall temperature that would be experienced in the capsule.

The test assembly was thermally cycled four times to specimen temperatures of (1) 1060°C, (2) 990°C, (3) 1040°C and (4) 1170°C. The heating and cooling cycles were 50 and 30 minutes respectively. On the last cycle, the filament touched the Kovar electrode which resulted in a localized melting and failure of the filament which terminated the test. During this event, the specimen experienced a transient temperature above 1450°C.

In spite of this event, only three small cracks were found in the lip area of the Lucalox specimen after the unit was disassembled. The cylindrical test area of the Lucalox was free of cracks. A metallic deposit was found on the lip area of the specimen; this was likely Kovar which deposited when the filament melted the electrode. All other parts of the assembly showed no changes.

Calculations based on the test data indicated that up to 24 w/cm^2 were transferred through the Lucalox specimen. A filament input power of 320 watts was recorded when the Kovar temperature was 1090°C. Only radiant heating from the filament was used. Average heat transferred through the specimen was estimated to be 192 watts. Calculations indicated that approximately 52 watts were radiated from the surface of the vacuum can to the bell jar wall. The difference was dissipated as end losses. A Δt of 50°C was measured during the test across the Kovar-molybdenum electrodes.

A temperature profile was calculated without the gamma heat, using the Kovar temperature reached during the first cycle and the estimated 192 watts transferred across the specimen. The estimated temperature drop of 55°C for contact resistances in the electrode assembly was not included in the calculated curve. When the test assembly was brought to

temperature (1st cycle) the temperature profile was plotted and is shown in Figure A. 2, in dotted lines. The temperature difference at surface 4 confirmed that the 55°C contact resistance estimate was conservatively high. Actual contact resistance whown by this test was approximately 20°C as shown at surface 3 in Figure A. 2. In this experiment no heater power was supplied. From the test data with the Kovar temperature at 400°C the Δt across the electrodes was 140°C. This was expected since at this temperature the parts had not expanded to reduce thermal contact resistance.

During thermal cycling, the electrometer was connected to the direct potential leads from the Kovar and molybdenum electrodes through a vacuum seal in the bell jar. A coaxial cable was used from the bell jar to the electrometer. However, in this test electrical interference was noted and was traced to the a-c power to the filament, the temperature recorder, the vac ion gage, and other a-c sources in the Laboratory. The actual capsule had been designed to eliminate as much interference as possible by shielding. And most significant was that the in-pile capsule was not heated with an a-c filament. Thermionic emission probably caused some measuring problems with this out-of-pile experiment.

A d-c power supply was used to apply 10, 20 and 28 V across the specimen and the resulting current was recorded by the electrometer. The resistance was calculated from plus and minus readings correcting for the generated voltage. This data was plotted as the log resistivity as a function of temperature for alumina and are presented in Figure A. 3. Due to the electrical interference problem, the data was scattered. The band drawn can be compared to the band for general alumina resistivity data taken in air which is also included in the figure. The vacuum data appeared to be higher at the higher temperature. The possibility that Lucalox would have a higher resistivity at temperature in a vacuum than in air was not surprising since

Figure A.2.

NASA INSULATOR IRRADIATION - THERMAL TEST TEMPERATURE PROFILE

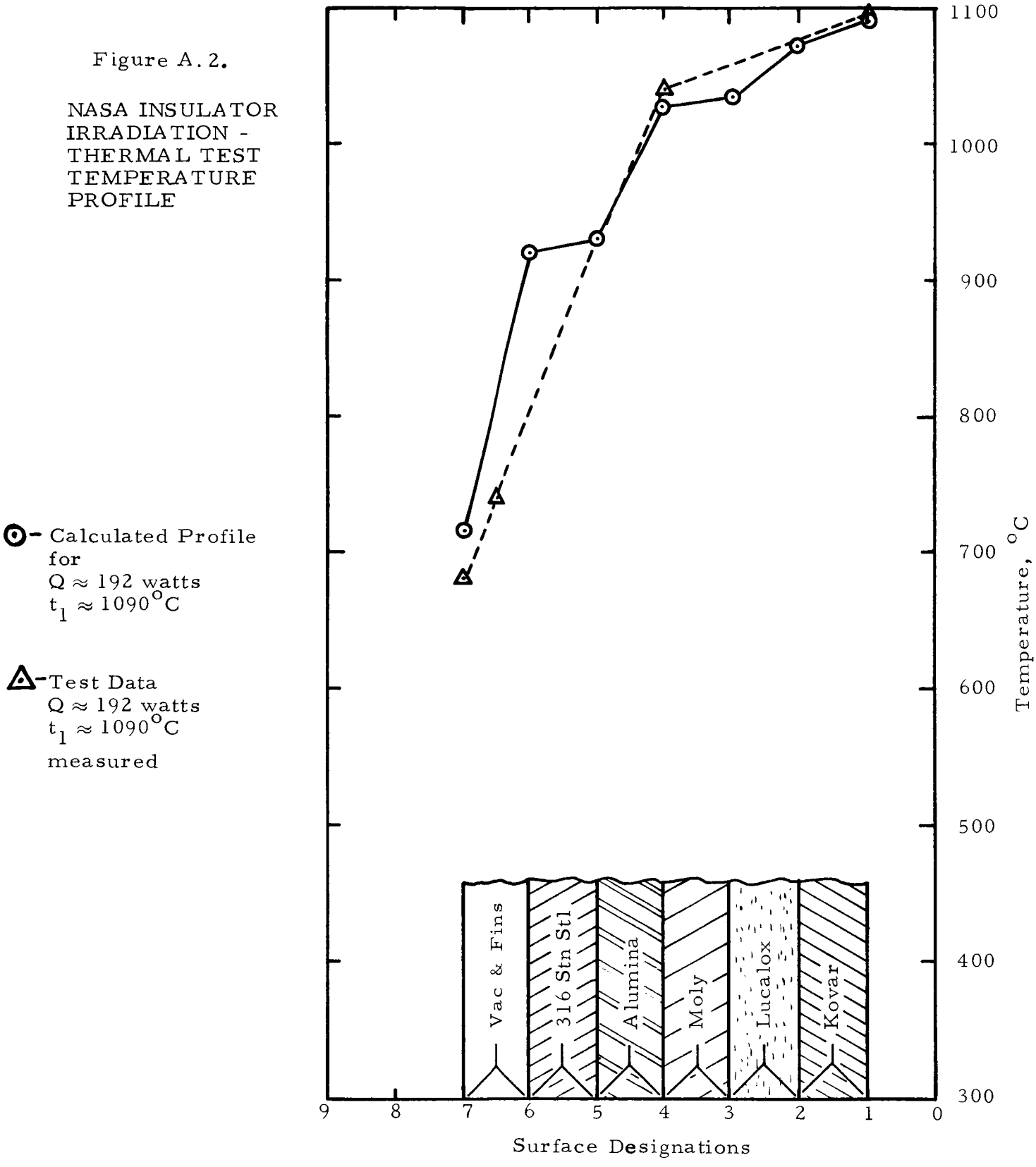

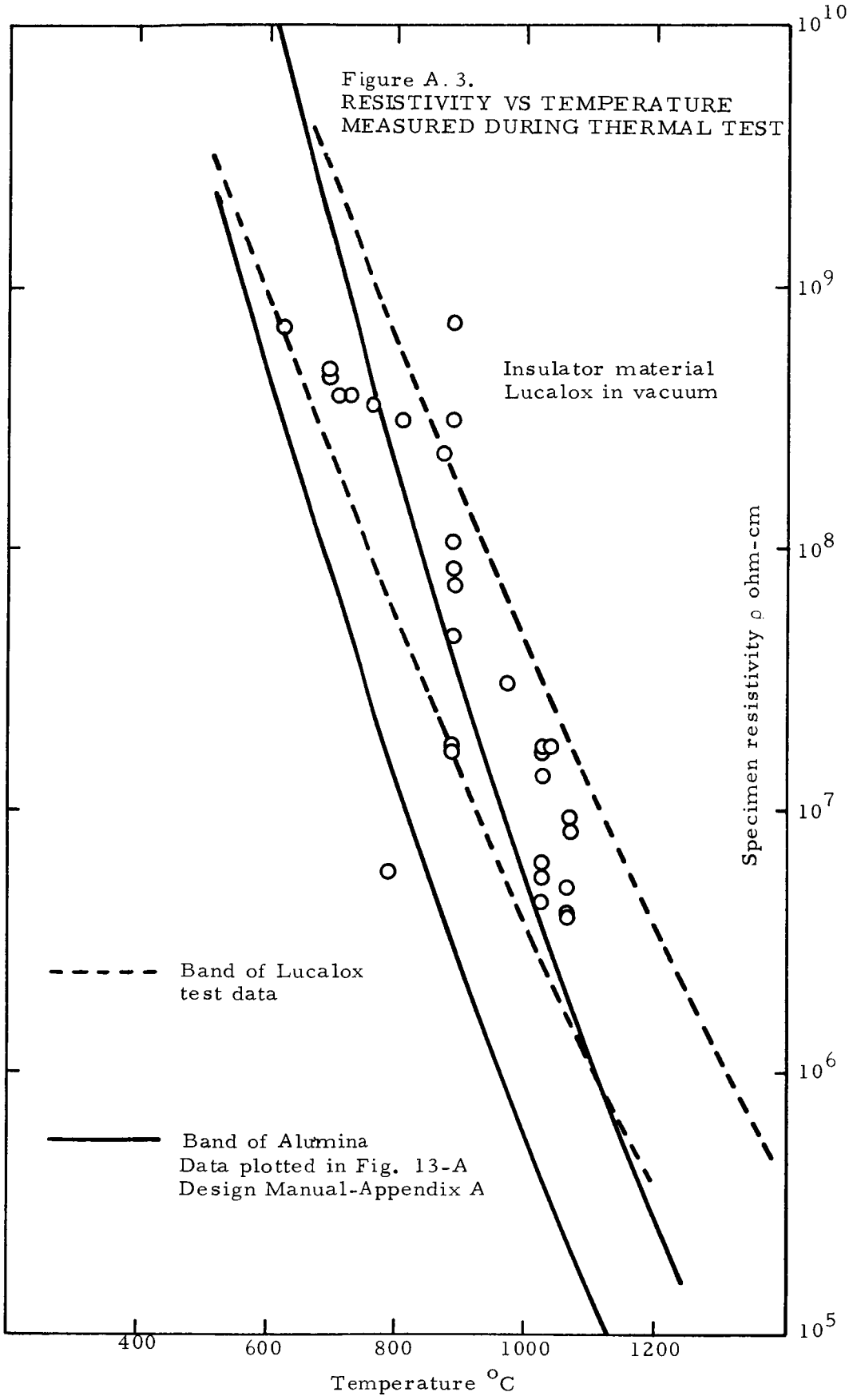
Figure A. 3.
RESISTIVITY VS TEMPERATURE
MEASURED DURING THERMAL TEST
Insulator material
Lucalox in vacuum
Band of Lucalox
test data
Band of Alumina
Data plotted in Fig. 13-A
Design Manual-Appendix A
Specimen resistivity ρ ohm-cm
10^{10}
10^{9}
10^{8}
10^{7}
10^{6}
10^{5}
400
600
800
1000
1200
Temperature °C

in vacuum condition would eliminate some possible surface and ionization effects. The ρ that could be calculated from these data were not highly accurate. However, this test was designed primarily as a thermal expansion and heat transfer experiment to confirm design calculations for the irradiation capsule.

Out-of-Pile Electrical Resistivity Measurements of Lucalox

A specimen assembly was made identical to that shown in Figure 5, while the Lucalox specimen itself was from the same lot to be used in the in-pile test. The specimen assembly was instrumented and inserted in a horizontal position in the center of a tube furnace; it was held by a long alumina tube which contacted the furnace walls only at one end where the temperature was $< 200^{o}$C. The two voltage leads were taken out opposite ends of the furnace so that no leakage across hot insulators was possible. The atmosphere in the furnace was flowing argon with between 5 and 9 ppm oxygen content throughout the experiment. Temperatures were measured with thermocouples. Electrical resistivity was measured using a Wheatstone Bridge for most determinations. Occasional cross-checks were made by a d.c. 2-probe method using voltages of 0 ± 6.7 volts. One volt-amp curve was obtained using voltages between 0 and + 400 volts.

In order to evaluate the effects of contact resistance and to determine if failure would occur as a result of the thermal expansion mismatches, a second specimen assembly was fabricated using the same Lucalox specimen that was used in the first experiment. This assembly, however, was not typical of the ones to be used in the in-pile test in that it was designed with closest fit dimensions possible which were necessary to achieve the objectives of the test.

The log of electrical resistivity as a function of temperature is plotted in Figure A.4 for the in-pile prototype specimen assembly. The initial heat up data probably represents surface contamination. This contaminant appeared to be driven off above 700°C and the specimen was heated to the isothermal test temperature of 990 ± 5°C. The specimen was held at temperature for 12 hours; a small change occurred in the electrical resistivity during the first hour and thereafter no further changes were observed. Resistivity measurements were taken on the cool down cycle to 675°C; below this temperature the resistance was too high to measure accurately.

The second specimen assembly was tested at 973°C after a heating period of three days to test temperature. The calculated resistivity measurements (also shown in Figure A.4) yielded data that was essentially identical to that for the in-pile prototype assembly. On the basis of these measurements, it was concluded that the contact resistance was not appreciable and would not influence the in-pile test results.

Four Probe Electrical Resistivity Measurements of Lucalox

After the irradiation of the Lucalox specimens, the question of electrical contact resistance was again raised. In order to obtain further information on this item, a four probe electrical resistivity measurement of Lucalox was performed. Molybdenum was metallized to the Lucalox sample to eliminate the mechanical specimen-electrode interface that was established by pressure contact. During the first measurements, the molybdenum electrode was partially oxidized and the electrical results show a variation with the heating and cooling portion of the curve. These data indicate that the bond between the molybdenum and Lucalox was parted, and therefore, the results were not conclusive.

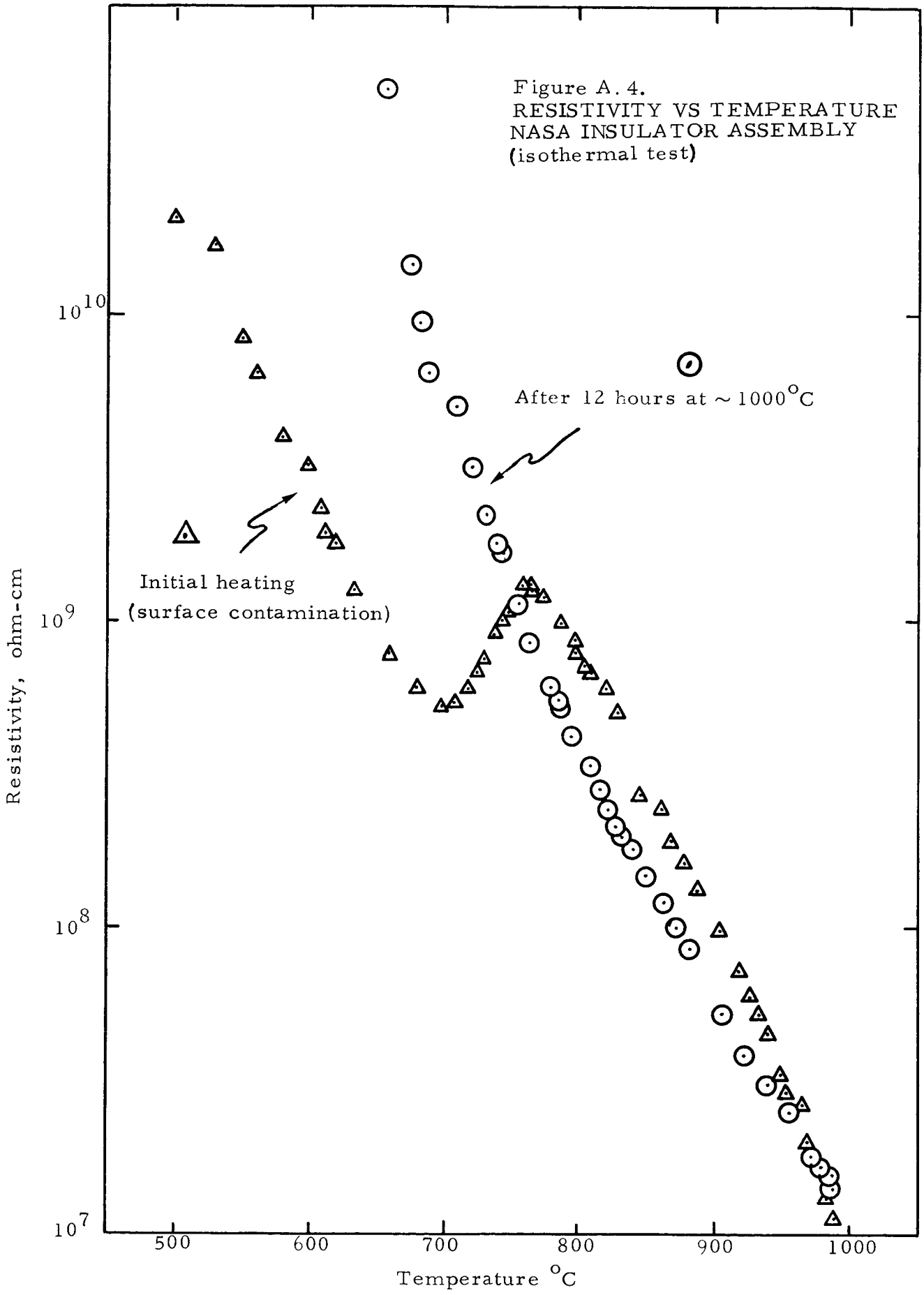
Figure A. 4.
RESISTIVITY VS TEMPERATURE
NASA INSULATOR ASSEMBLY
(isothermal test)
After 12 hours at ~ 1000°C
Initial heating
(surface contamination)
Resistivity, ohm-cm
10^10
10^9
10^8
10^7
500
600
700
800
900
1000
Temperature °C

Electrical Resistivity Measurements of Wesgo Alumina

Electrical resistivity measurements of the alumina isolation insulator were made over a range of temperatures. The alumina used for this application was Wesgo 97.5% pure alumina. A specimen, 0.049 inch by 0.433 inch was cut from the as-received right cylinder stock. The specimen was metallized with platinum and platinum foil was then brazed to the sample. Platinum leads were spot welded to the foil. The specimen was centered in a vertical resistance furance and tested in an argon atmosphere. The techniques described in the previous section were used to measure the electrical properties of the Wesgo 97.5.

The values of electrical resistivity are plotted as a function of temperature in Figure A.5. These results are in general agreement with much of the published literature on alumina. Based on these measured values, the material was acceptable for use as the isolation insulator member of the capsule.

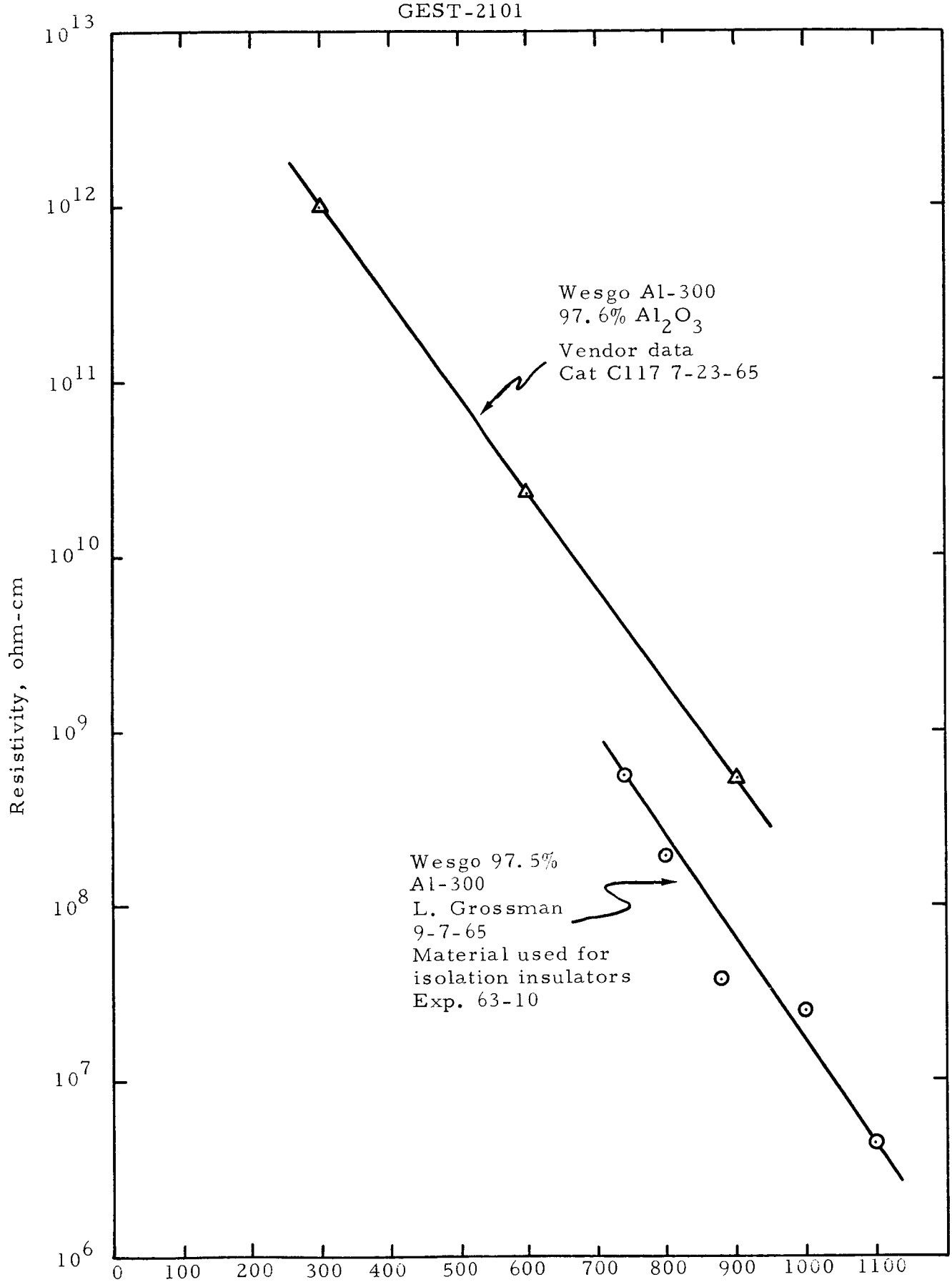

Figure A.5. ELECTRICAL RESISTIVITY OF WESGO 97.5%

APPENDIX B

DATA PLOTS OF THE IN-PILE MEASUREMENTS

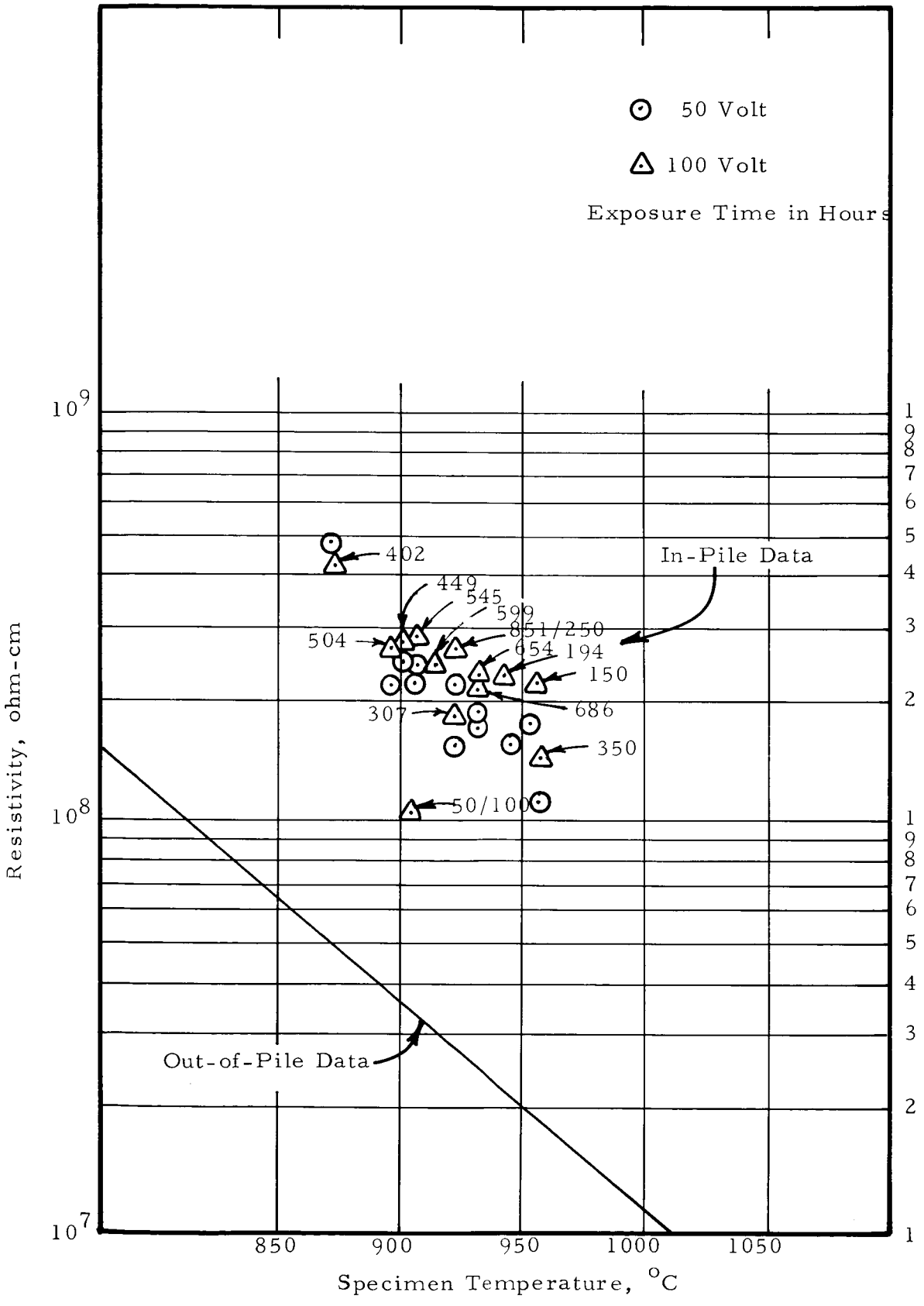

Figure B.1. RESISTIVITY VS TEMPERATURE FOR VARIOUS EXPOSURES, SPECIMEN NO. 1

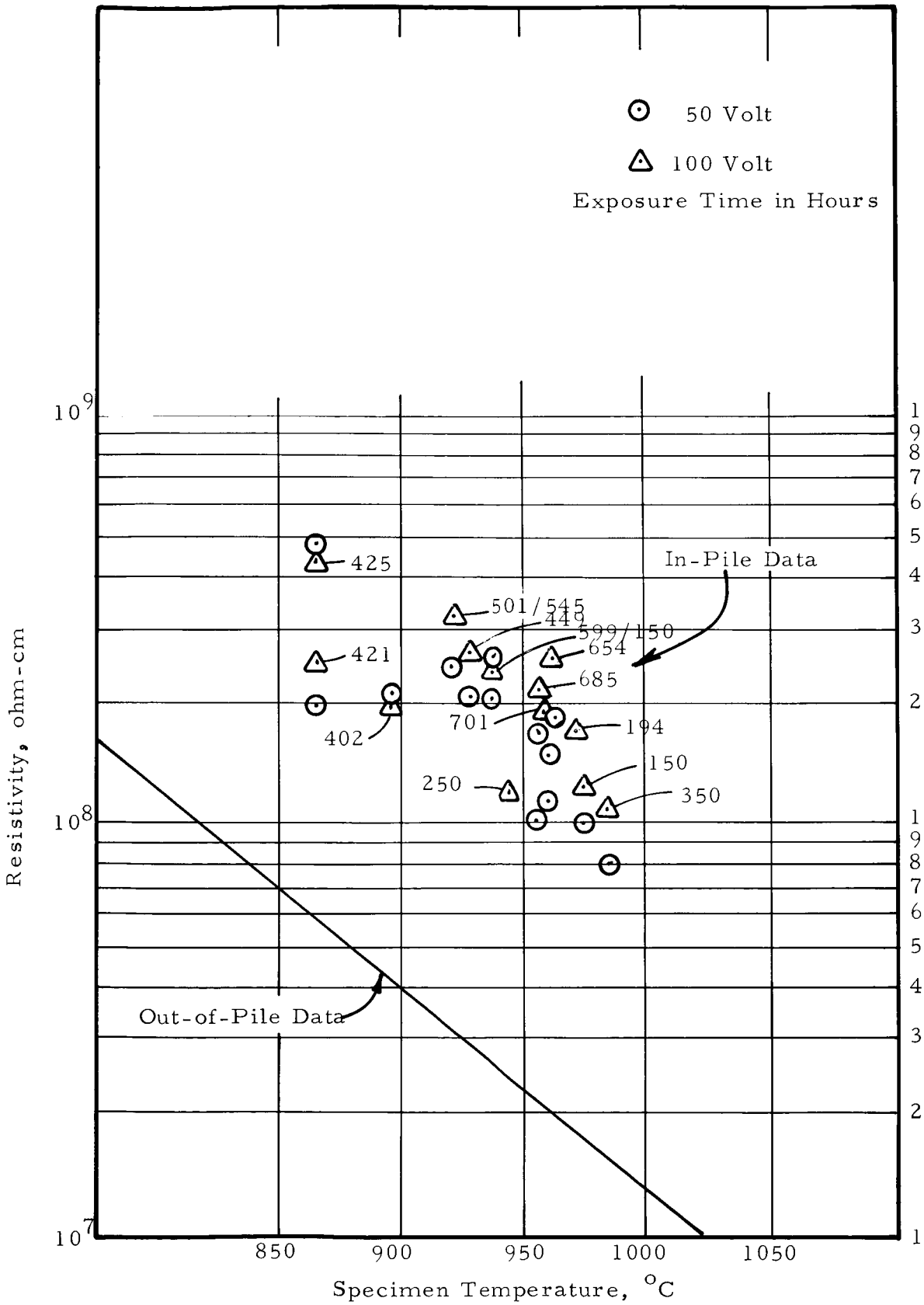

Figure B.2. RESISTIVITY VS TEMPERATURE FOR VARIOUS EXPOSURES, SPECIMEN NO. 2

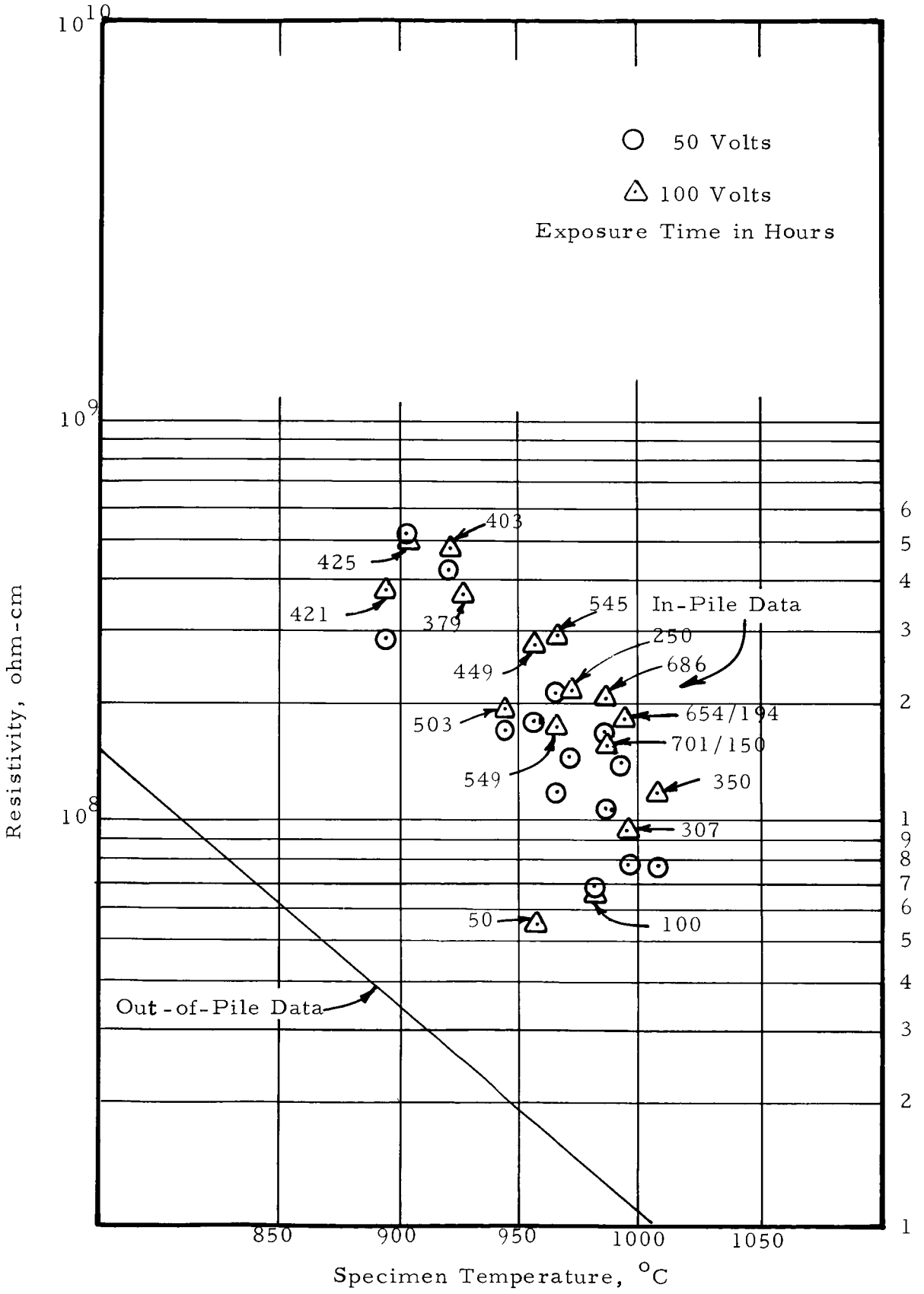

Figure B. 3. RESISTIVITY VS TEMPERATURE FOR VARIOUS EXPOSURES, SPECIMEN NO. 3

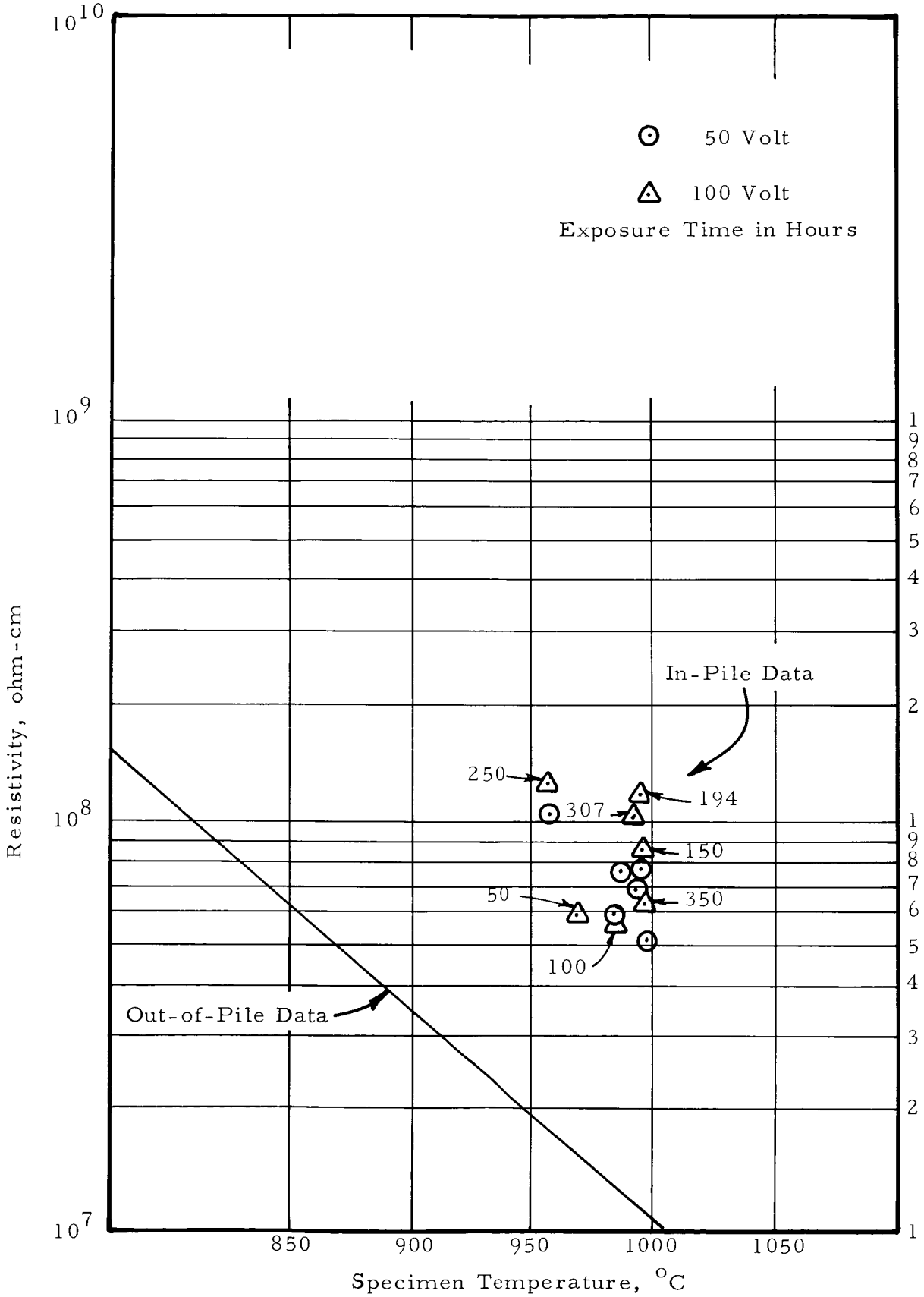

Figure B.4. RESISTIVITY VS TEMPERATURE FOR VARIOUS EXPOSURES, SPECIMEN NO. 4

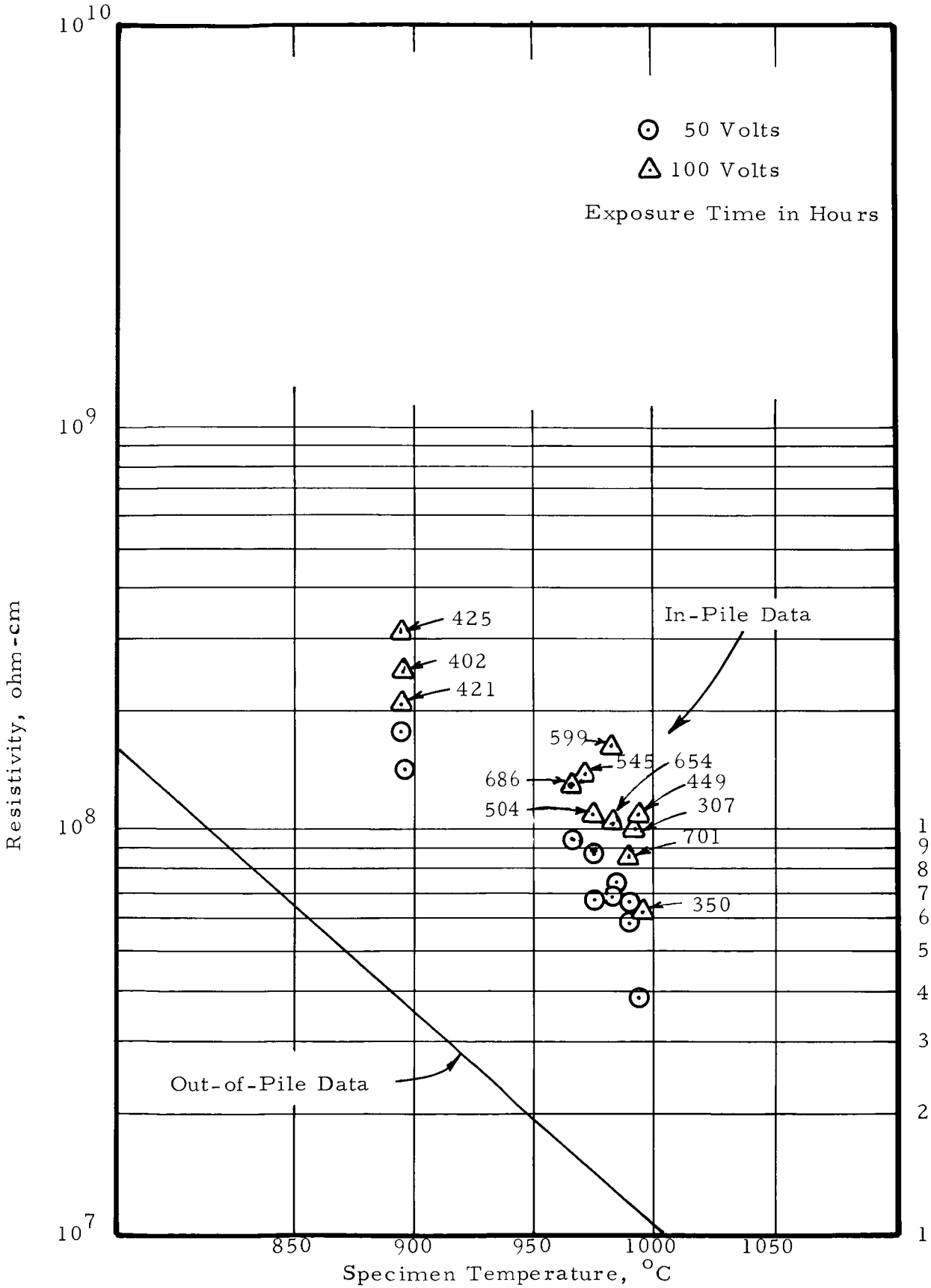

Figure B.5. RESISTIVITY VS TEMPERATURE FOR VARIOUS EXPOSURES, SPECIMEN NO. 5

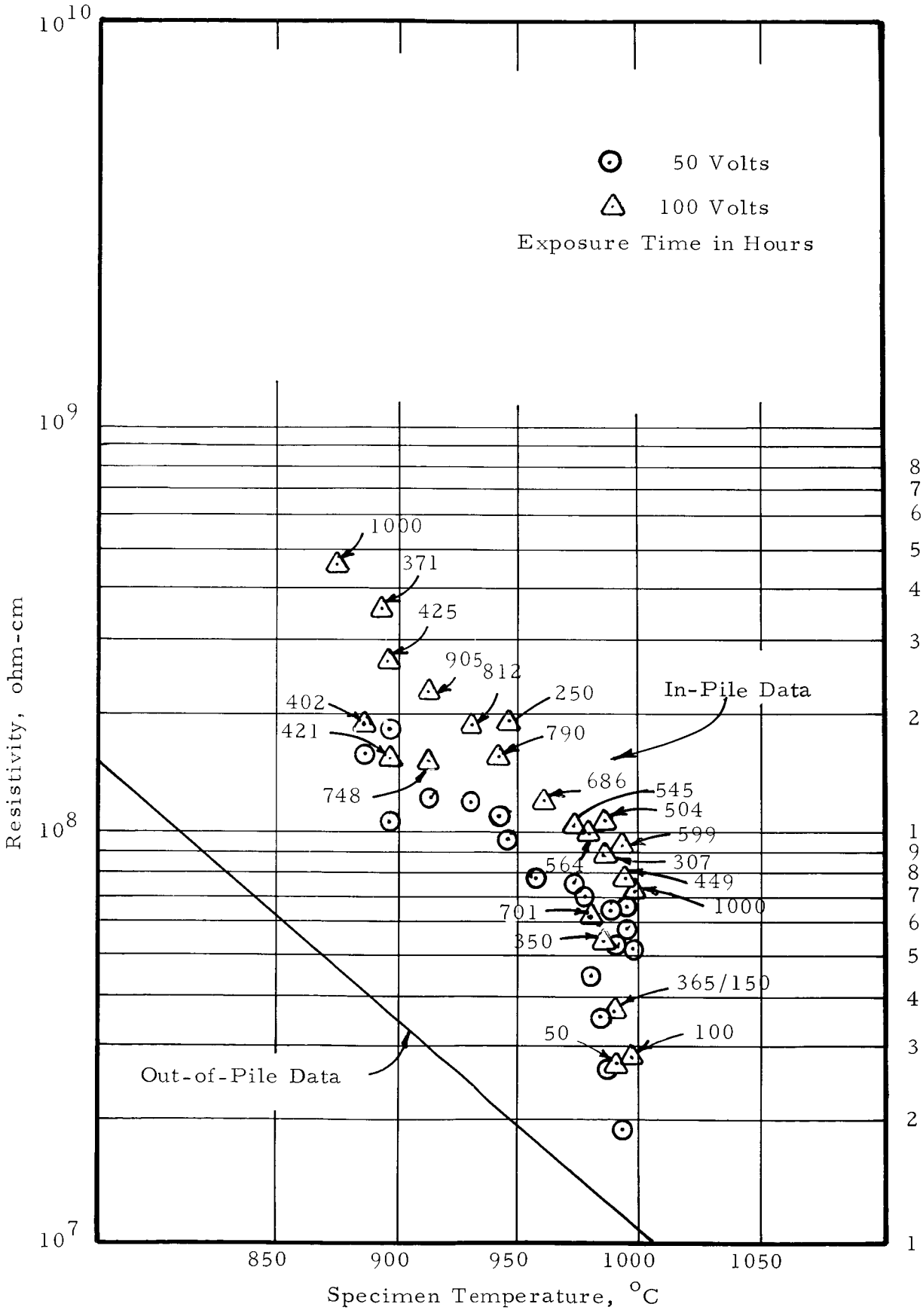

Figure B.6. RESISTIVITY VS TEMPERATURE FOR VARIOUS EXPOSURES, SPECIMEN NO. 6

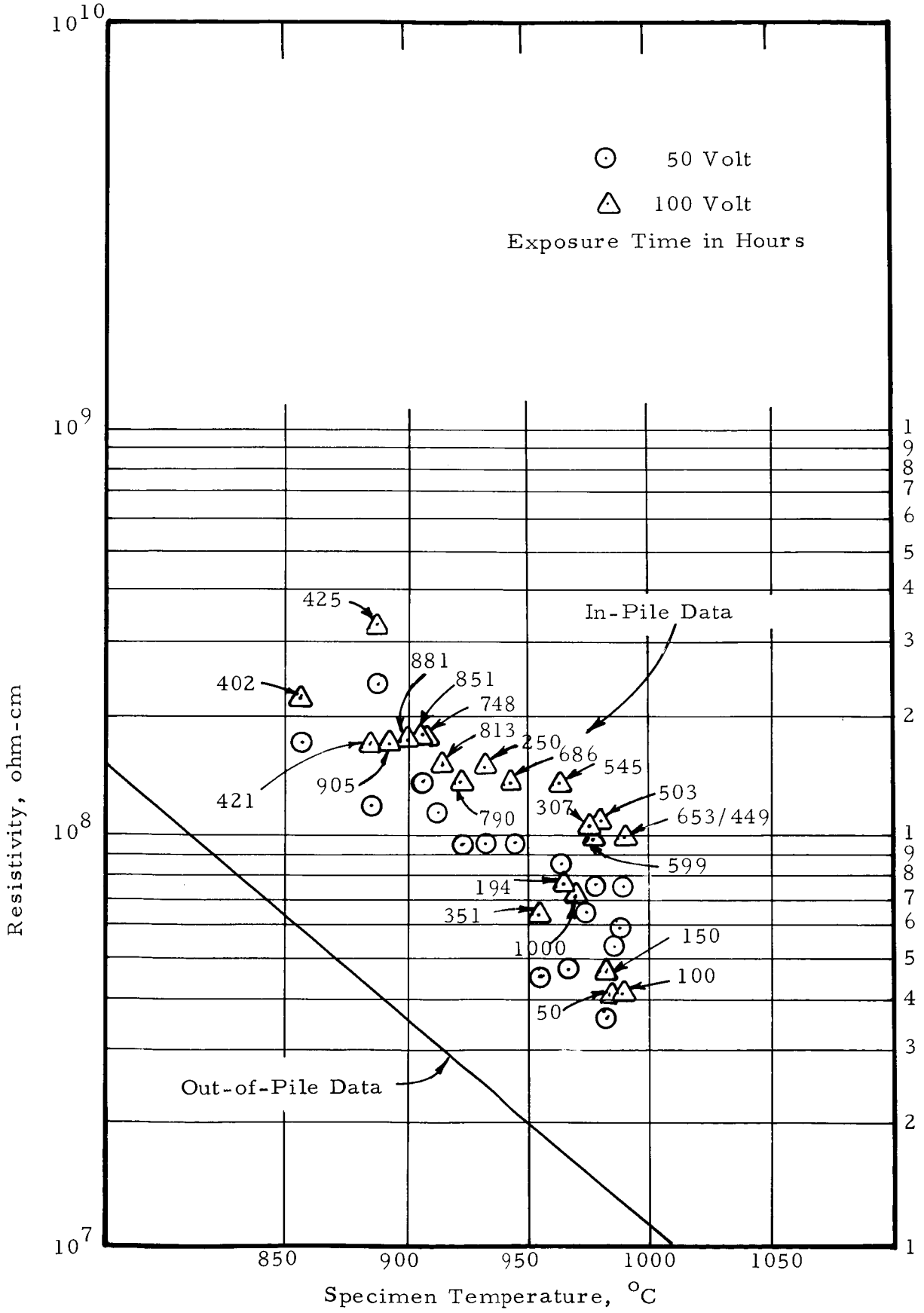

Figure B. 7. RESISTIVITY VS TEMPERATURE FOR VARIOUS EXPOSURES, SPECIMEN NO. 7

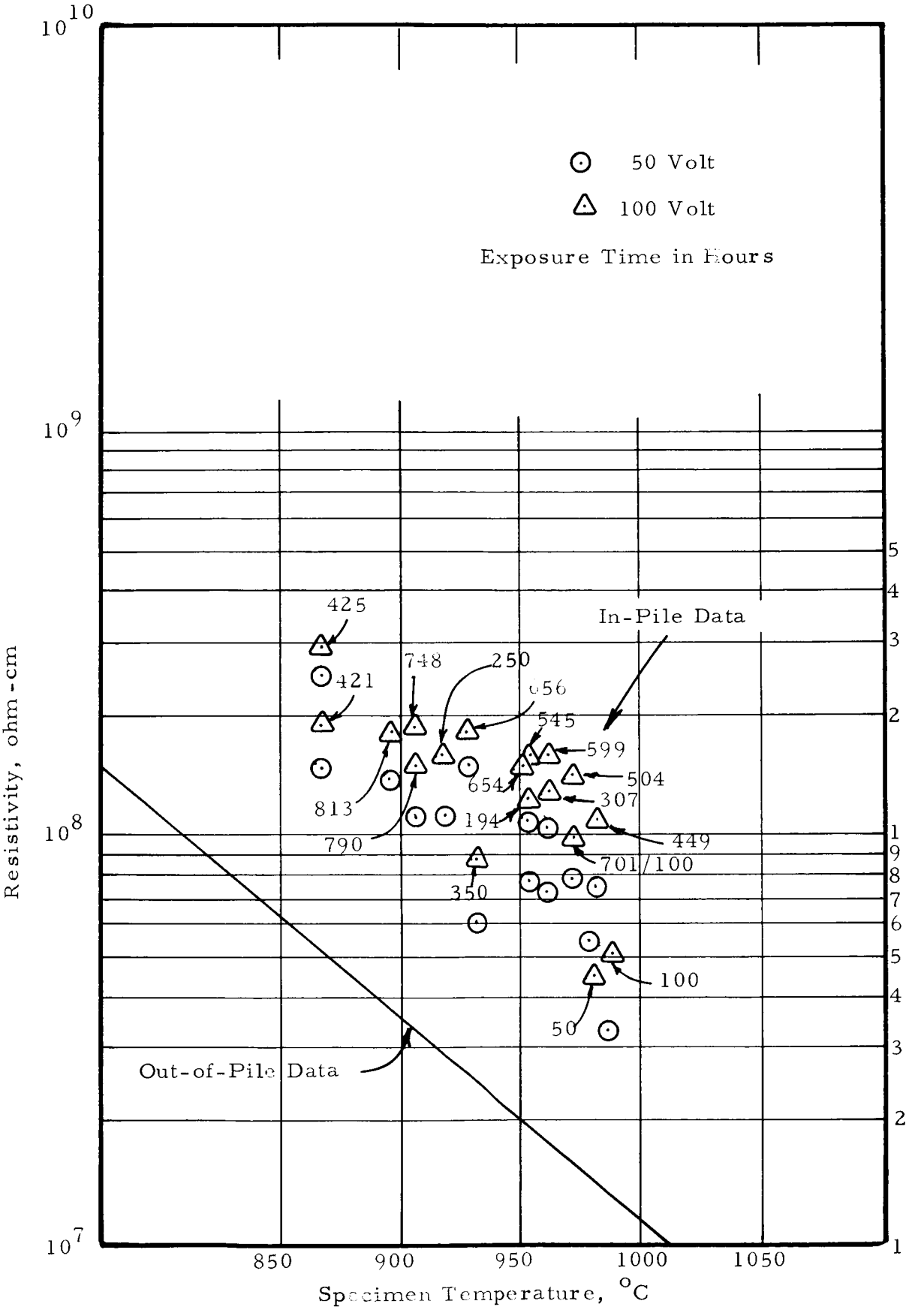

Figure B. 8. RESISTIVITY VS TEMPERATURE FOR VARIOUS EXPOSURES, SPECIMEN NO. 8

REFERENCES

A. References for Properties of High Purity Alumina

1. Cusack, "The Electrical & Magnetic Properties of Solids."
2. Ryshkewitch, "Oxide Ceramics."
3. Kohl, "Materials and Technology for Electron Tubes," Reinhold.
4. Materials and Design Engineer, Manual No. 208, July, 1963, Reinhold.
5. Young, "Materials and Processes," Wiley.
6. Coors, General Electric, and Wesgo, Literature on High Purity Alumina.
7. Am. Ceramic Soc. Bulletin, April, 1957, Vol. 36 No. 4, 133
8. Ceramic Data Book, Ind. Publications, Inc.
9. Campbell, "High Temperature Technology," Wiley.
10. Kingery, "Property Measurements at High Temperature," Wiley.
11. Kingery, "Introduction to Ceramics."
12. Keilliotz, G.W., Lee, J.E., Jr. and Moore, R.E., "Properties of Magnesium, Aluminum, and Beryllium Oxide Compacts Irradiated to Fast-Neutron Doses Greater than 10^{21} neutrons cm^{-2} at 150, 800, and 1100°C," Reactor Chemistry Division, Oak Ridge National Lab.
13. Grossman, L.N., "Thermophysical Properties of Some Materials," General Electric Company, GEAP 3734, Vallecitos Nuclear Center.
14. Hickman, B.S. and Walker, D.G., "The Effect of Neutron Irradiation on Aluminum Oxide," J. of Nuc. Matls. 18 (1966), 197-205.
15. Dau, G.J. and Davis, M.V., "The Electrical Conductivity of Alumina at Temperatures in a Reactor Environment," Nuclear Science and Engineering 21, 30-33 (1965).
16. Bockris, MacKenzie, and White, "Physicochemical Measurements at High Temperature," Butterworth.
17. "Temperature, Its Measurement and Control," Am. Inst. of Physics, Reinhold.
18. Champion, J.A., "The Electrical Conductivity of Single Crystal Alumina," Brit. J. Appl. Phys., 1964, Vol. 15.
19. Creamer, R.H. and Harrop, P.J., "The High Temperature Electrical Conductivity of Single Crystal Alumina," Brit. J. Appl. Phys., 1963, Vol. 14.
20. Cohen, J., "Electrical Conductivity of Alumina," Sylvania Research Laboratories, Bayside, N.Y., Ceramic Bulletin, Vol. 38, No. 9, 1959, 441.

21. Dau, G. J., Davis, M. V. and Haidler, W. B., "Electrical Conductivity of Alumina in Radiation Fields," University of Arizona, presented at 1964 Winter Meeting ANS, San Francisco, California.

22. Henry, J. J., "Contact Resistance", AEC Report MIT 2079-2, Thesis, June, 1964.

23. "Electrometer Measurements," Keithley Instruments, Inc., Instruments and Control Systems, Vol. 35.

24. "Electrical Properties of Single Crystal and Polycrystalline Alumina at High Temperature," J. Am. Cer. Soc. 44 (a), 459 (1961).

25. General Electric Company Vendor Literature, L-2-R, Polycrystalline Lucalox Ceramic Lamp Glass Department, General Electric Company, Jan. 1963.

26. "Translucent Alumina Stays Strong to 3600°F," Materials in Design Magazine, Reinhold, April, 1963.

27. "Resistivity Characteristics of Some Ceramic Compositions above 1000°F," Am. Cer. Soc. Bulletin, Vol. 36, No. 4, 1957.

28. "A Simple DC Method for the Determination of the Electrical Resistance of Glass," J. Soc. Glass Tech., Vol. 39, 1955.

29. Gregory, T. L., "Irradiation of High Purity Alumina," paper was presented at Conf. on Applied Thermionic Tech., Germantown, Md., May, 1965, by D. L. Francis.

30. Crawford, Tripp, Weil, "The Electrical Behavior of Refractory Oxides," ARL 64-122, Aug. 1964.

31. Grossman, L. N., "Electrical Insulators and Spacers for Nuclear Thermionic Devices," GEST-2022, Contract NObs-88378, Feb., 1964.

32. Dawson, P. H., "Secondary Electron Emission Properties of Some Ceramics," GE 64RL-3775E, Sept., 1964.

33. Patrick, A. J., Stoddard, S. D., "Irradiation Damage to Ceramics and Metallic Ceramic Bonds, LA-DC-6822, May, 1965.

34. Dekker, A. J., "Solid State Physics," Prentice Hall.

35. Kittel, "Introduction to Solid State Physics," Wiley.

B. References relating to Capsule Design

36. McAdams, Heat Transmission, McGraw-Hill, 3rd ed.

37. Glasstone, Principles of Nuclear Reactor Engineering, VanNostrand.

38. Bonilla, Nuclear Engineering, McGraw-Hill.

39. Marks, Mechanical Engineer's Handbook, McGraw-Hill)

40. Tebo, "Selected Values of the Physical Properties of Various Materials," ANL-5914.

41. Goldsmith, Hirshhorn, and Waterman, Handbook of Thermal Physical Properties of Solid Materials, Armour Research.

42. Roark, Formulas for Stress and Strain, 3rd ed. McGraw-Hill.

43. Timoshenko, Strength of Materials, Part I.

44. ASME Pressure Vessel Code, Sec. VIII.

45. ASME Material Specifications, Sec. II.

46. ASM Metals Handbook

47. "Heat Transfer Manual," General Electric Research Laboratory, Schenectady, New York.

48. Kreith, Principles of Heat Transfer, International Text Book.

49. Bolt, Carrol, "Radiation Effects on Organic Material," Academic Press.

50. Faires, Thermodynamics, McMillian.

51. Request for Irradiation EC 62-07.

52. Design Manual and Hazards Analysis for Insulator Irradiation, PBR Experiment 63-10, March 5, 1964.

53. Operation Manual for Insulator Irradiation PBR Experiment 63-10, July 15, 1964.

DISTRIBUTION LIST

Aerojet General Nucleonics
San Ramon, California
Attn: K. Johnson (1)

Aerospace Corporation
El Segundo, California
Attn: Librarian (1)

Air Force Cambridge Research Center
(CRZAP)
L. C. Hanscom Field
Bedford, Massachusetts (1)

Air Force Systems Command
Aeronautical Systems Division
Flight Accessories Laboratory
Wright-Patterson AFB, Ohio
Attn: APIP-2/E. A. Wallis (1)

Allison Division
General Motors Corporation
Indianapolis 6, Indiana
Attn: T. F. Nagey (1)

Aracon Laboratories
Virginia Road
Concord, Massachusetts
Attn: S. Ruby (1)

Argonne National Laboratory
9700 South Cass Avenue
Argonne, Illinois
Attn: Aaron J. Ulrich (1)

Armour Research Foundation
10 West 35th Street
Chicago 16, Illinois
Attn: D. W. Levinson (1)

Astropower, Inc.
2121 Paularino Avenue
Newport Beach, California
Attn: Lou H. Mick (1)

Atomics International
P. O. Box 309
Canoga Park, California
Attn: Robert C. Allen (1)
Attn: Charles K. Smith (1)

The Babcock & Wilcox Company
1201 Kemper Street
Lynchburg, Virginia
Attn: Frank R. Ward (1)

Battelle Memorial Institute
505 King Avenue
Columbus 1, Ohio
Attn: David Dingee (1)
Attn: Don Keller (1)

Brookhaven National Laboratory
Upton, Long Island, New York
Attn: Dr. O. E. Swyer (1)

Bureau of Ships
Department of the Navy
Washington 25, D. C.
Attn: B. B. Rosenbaum (1)

CANEL Facility
Middletown, Connecticut
Attn: M. DeCrescente (1)

CANEL Project Office
US Atomic Energy Commission
P. O. Box 1102
Middletown, Connecticut (1)
Attn: H. Pennington

Consolidated Controls Corp.
Bethel, Connecticut
Attn: David Mende (1)

Douglas Aircraft Company
Missile & Space Engineering
Nuclear Research (AZ-260)
3000 Ocean Park
Santa Monica, California
Attn: A. DelGrosso (1)

Electro Optical Systems, Inc.
300 North Halstead Avenue
Pasadena, California
Attn: A. Jensen (1)

Ford Instrument Company
32-36 47th Avenue
Long Island City, New York
Attn: T. Jarvis (1)

General Atomic
P. O. Box 608
San Diego 12, California
Attn: R. W. Pidd (1)
Attn: W. Wright (1)
Attn: L. Yang (1)
Attn: A. Weinberg (1)

General Electric Company
Knolls Atomic Power Laboratory
Schenectady, New York
Attn: R. Ehrlich (1)

General Electric Company
Power Tube Division
One River Road
Schenectady, New York
Attn: D. L. Schaefer (1)

General Electric Company
Nuclear Materials and Propulsion Opn.
P. O. Box 15132
Cincinnati 15, Ohio
Attn: J. A. McGurty (1)

General Electric Company
Research Laboratory
Schenectady, New York
Attn: V. C. Wilson (1)

General Motors Corporation
Research Laboratories
Warren, Michigan
Attn: F. E. Jamerson (1)

General Telephone & Electronics
Laboratories, Inc.
Bayside 60, New York
Attn: R. Steinitz (1)

Hughes Research Laboratories
3011 Malibu Canyon Road
Malibu, California
Attn: R. C. Knechtli (1)

Institute for Defense Analyses
400 Army-Navy Drive
Arlington, Virginia 22202
Attn: R. C. Hamilton (1)

International Telephone and
Telegraph Laboratories
Fort Wayne, Indiana
Attn: Donald K. Coles (1)

Jet Propulsion Laboratory
California Institute of Technology
4800 Oak Grove Drive
Pasadena, California
Attn: Arvin Smith (1)
Attn: Peter Rouklove (1)

Los Alamos Scientific Laboratory
P. O. Box 1663
Los Alamos, New Mexico (2)

Marquardt Corporation
Astro Division
16555 Saticoy Street
Van Nuys, California
Attn: A. N. Thomas (1)

Martin Nuclear
Division of Martin-Marietta Corp.
P. O. Box 5042
Middle River 3, Maryland
Attn: W. J. Leyendahl (1)

Massachusetts Institute of Technology
Cambridge, Massachusetts
Attn: Wayne B. Nottingham (1)

National Aeronautics & Space Adm.
Western Operations Office
150 Pico Boulevard
Santa Monica, California
Attn: Fred Glaski (1)

National Aeronautics & Space Adm.
Manned Spacecraft Center
Houston, Texas
Attn: Librarian (1)

National Aeronautics & Space Adm.
1512 H Street, N.W.
Washington 25, D. C.
Attn: Fred Schulman (1)
Attn: James J. Lynch (1)
Attn: George Deutsch (1)
Attn: Walter Scott (1)

National Aeronautics & Space Adm.
Lewis Research Center
21000 Brookpark Road
Cleveland, Ohio 44135
Attn: Roland Breitwieser (C&EC) (1)
Attn: Bernard Lubarsky (SPSD) (1)
Attn: Robert Migra (NRD) (1)
Attn: Gerald R. Brendel (SPSD) (3)
Attn: James J. Ward (SPSD) (1)
Attn: Herman Schwartz (SPSD) (1)
Attn: H. B. Probst (M&S) (1)
Attn: J. F. Mondt (SPSD) (1)
Attn: T. A. Moss (SPSD) (1)
Attn: Frank Rzasa (SPSPS) (1)
Attn: R. Mather (SPSD) (1)
Attn: Report Control Office (1)

National Aeronautics & Space Adm.
Marshall Space Flight Center
Huntsville, Alabama
Attn: Library (1)

National Aeronautics & Space Adm.
Scientific & Technical Information Facility
Box 5700
Bethesda 14, Maryland
Attn: NASA Representative (2)

National Bureau of Standards
Washington, D. C.
Attn: G. F. Rouse (1)

Oak Ridge National Laboratory
Oak Ridge, Tennessee
Attn: Library (1)

Office of Naval Research
Power Branch
Dept. of the Navy
Washington 25, D. C.
Attn: Cmdr. J. J. Connelly, Jr. (1)

Power Information Center
University of Pennsylvania
Moore School Building
200 South 33rd Street
Philadelphia 4, Pennsylvania (1)

Pratt & Whitney Aircraft Corp.
East Hartford 8, Connecticut
Attn: William Lueckel (1)
Attn: Ron Cohen (1)

Radiation Effects Information Center
Battelle Memorial Institute
505 King Avenue
Columbus 1, Ohio
Attn: R. E. Bowman (1)

Radio Corporation of America
David Sarnoff Research Center
Princeton, New Jersey
Attn: Karl G. Hernqvist (1)
Attn: Paul Rappaport (1)

Radio Corporation of America
Electron Tube Division
Lancaster, Pennsylvania
Attn: Fred Block (1)

The Rand Corporation
1700 Main Street
Santa Monica, California
Attn: Librarian (1)

Republic Aviation Corporation
Farmingdale, Long Island, New York
Attn: Alfred Schock (1)

Space Technology Laboratories
Los Angeles 45, California
Attn: Librarian (1)

Texas Instruments, Inc.
P. O. Box 5474
Dallas 22, Texas
Attn: R. A. Chapman (1)

Thermo Electron Engineering Corp.
85 First Avenue
Waltham 54, Massachusetts
Attn: George Hatsopoulos (1)
Attn: Ned Rasor (1)

Thompson Ramo Wooldridge, Inc.
7209 Platt Avenue
Cleveland 4, Ohio
Attn: W. J. Leovic (1)

Union Carbide Corporation
Parma Research Center
12900 Snow Road
Parma, Ohio
Attn. Librarian (1)

United Aircraft Corporation
Research Laboratories
East Hartford, Connecticut
Attn: R. Meyerand (1)

United Nuclear Corporation
5 New Street
White Plains, New York
Attn: Al Strasser (1)

U. S. Army Signal R&D Laboratory
Fort Monmouth, New Jersey
Attn: Emil Kittil (1)

U. S. Atomic Energy Commission
Fuels & Materials Development Branch
Germantown, Maryland
Attn: Socrates Christopher (1)

U. S. Atomic Energy Commission
Division of Reactor Development
Washington 25, D. C.
Attn: Auxiliary Power Branch (1)
Attn: Direct Conversion Branch (1)
Attn: Army Reactor Water Systems Branch (
Attn: Isotopic Branch (1)
Attn: SNAP Reactors Branch (1)

U. S. Atomic Energy Commission
Technical Reports Library
Washington 25, D. C.
Attn: J. M. O'Leary (3)

U. S. Atomic Energy Commission
Dept. of Technical Information Extension
P. O. Box 62
Oak Ridge, Tennessee (3)

U. S. Atomic Energy Commission
San Francisco Operations Office
2111 Bancroft Way
Berkeley 4, California
Attn: Reactor Division (1)

U. S. Naval Research Laboratory
Washington 25, D. C.
Attn: George Haas (1)
Attn: Library (1)

University of Wisconsin
Madison, Wisconsin
Attn: Harold W. Lewis (1)

Westinghouse Electric Corporation
Aerospace Department
Lima, Ohio
Attn: Harry Gray (1)

Westinghouse Electric Corporation
Research Laboratories
Pittsburgh, Pennsylvania
Attn: R. J. Zellweg (1)